Geodetic observations for constraining mantle processes in Antarctica

Scheinert, Mirko; Engels, Olga; Schrama, Ernst J.O.; van der Wal, Wouter; Horwath, Martin

DOI
10.1144/M56-2021-22

Publication date
2023

Document Version
Final published version

Published in
Geological Society Memoir

Citation (APA)
Scheinert, M., Engels, O., Schrama, E. J. O., van der Wal, W., & Horwath, M. (2023). Geodetic observations for constraining mantle processes in Antarctica. *Geological Society Memoir*, *56*(1), 295-313. https://doi.org/10.1144/M56-2021-22

Geodetic observations for constraining mantle processes in Antarctica

Mirko Scheinert[1]*, Olga Engels[2], Ernst J. O. Schrama[3], Wouter van der Wal[3,4] and Martin Horwath[1]

[1]Institut für Planetare Geodäsie, Technische Universität Dresden, Helmholtzstraße 10, 01069 Dresden, Germany

[2]Institute of Geodesy and Geoinformation, University of Bonn, Nussallee 17, 53115 Bonn, Germany

[3]Faculty of Aerospace Engineering, Delft University of Technology, Kluyverweg 1, 2629 HS Delft, The Netherlands

[4]Faculty of Civil Engineering, Delft University of Technology, Stevinweg 1, 2628 CN Delft, The Netherlands

MS, 0000-0002-0892-8941; OE, 0000-0001-8521-3475; EJOS, 0000-0002-9654-4082; WW, 0000-0001-8030-9080; MH, 0000-0001-5797-244X

*Correspondence: Mirko.Scheinert@tu-dresden.de

Abstract: Geodynamic processes in Antarctica such as glacial isostatic adjustment (GIA) and post-seismic deformation are measured by geodetic observations such as global navigation satellite systems (GNSS) and satellite gravimetry. GNSS measurements have comprised both continuous measurements and episodic measurements since the mid-1990s. The estimated velocities typically reach an accuracy of 1 mm a^{-1} for horizontal velocities and 2 mm a^{-1} for vertical velocities. However, the elastic deformation due to present-day ice-load change needs to be considered accordingly.

Space gravimetry derives mass changes from small variations in the inter-satellite distance of a pair of satellites, starting with the GRACE (Gravity Recovery and Climate Experiment) satellite mission in 2002 and continuing with the GRACE-FO (GRACE Follow-On) mission launched in 2018. The spatial resolution of the measurements is low (about 300 km) but the measurement error is homogeneous across Antarctica. The estimated trends contain signals from ice-mass change, and local and global GIA signals. To combine the strengths of the individual datasets, statistical combinations of GNSS, GRACE and satellite altimetry data have been developed. These combinations rely on realistic error estimates and assumptions of snow density. Nevertheless, they capture signals that are missing from geodynamic forward models such as the large uplift in the Amundsen Sea sector caused by a low-viscous response to century-scale ice-mass changes.

Several geodynamic processes occurring in the Earth's mantle manifest in geodetic observations in Antarctica such as global navigation satellite systems (GNSS: comprising GPS, GLONASS, Galileo, BeiDou and further systems), time-variable gravity and satellite altimetry. These include surface-loading processes from past ice-thickness changes, post-seismic deformation and possible dynamic topography. The geodetic observations are becoming more numerous because of continuous coverage from satellite measurements and increasing efforts to place GNSS antennas on bedrock in Antarctica. At the same time, measurements are becoming more accurate with increasing instrument precision and better corrections (King *et al.* 2010). Moreover, geodynamic processes are visible as secular trends, which means that with longer time series from GNSS or satellite measurements the signal/noise ratio of geodynamic signals increases. The dominant problem in observing geodynamic processes with geodetic observations is that several processes are mixed; uplift or gravity rates are influenced by current ice unloading, past ice-thickness changes and post-seismic changes. Therefore, several studies have been dedicated to disentangling the processes by using models as well as further non-geodetic data (e.g. firn compaction: Ligtenberg *et al.* 2011; rheological parameters based on seismic tomography: van der Wal *et al.* 2015). Recent studies have had success in constraining the glacial isostatic adjustment (GIA) process and post-seismic deformation (Barletta *et al.* 2022, this volume). This chapter provides an overview of the main geodetic data types, their strengths and weaknesses, and main results.

Measurements collected by permanently or temporarily installed GNSS receivers are most valuable since they allow coordinates and coordinate changes to be accurately inferred, and, thus, the time-variable geometry of the Earth's surface to be determined (King *et al.* 2010). For our purpose, we are interested in geodetic GNSS equipment with the antenna stably placed on bedrock and the receiver permanently recording data (permanent station) or in certain observation periods (campaign station). An overview of measurements and insights is presented in the following section. Time-variable gravity data from the GRACE (Gravity Recovery and Climate Experiment) and GRACE-FO (GRACE Follow-On) missions are discussed in the 'Temporal gravity field variations from satellite gravimetry' section, while the static gravity measurements are discussed by Pappa and Ebbing (2021, this volume). Further constraints for modelling GIA may be inferred from relative sea-level curves where they can be unequivocally identified and dated (e.g. Peltier 1998). However, Antarctica near-field relative sea-level data are scarce and are not able to provide a similar level of information as GNSS (e.g. Ivins and James 2005).

To address the problem of superposition of processes, several studies have produced combinations of measurements, each of which has a different sensitivity to surface and solid Earth processes (e.g. Riva *et al.* 2009; Groh *et al.* 2014; Gunter *et al.* 2014; Martín-Español *et al.* 2016*b*). These measurements can include GRACE-derived temporal gravity changes, surface changes from radar and/or laser altimetry, and position changes from GNSS. The combinations increased the constraints on the GIA process and have become known as 'empirical' or 'inverse' GIA models. These will be reviewed in the 'Results on mantle-related processes from geodetic data combination' section. The chapter concludes with a summary of the state of the art and an outlook for possible improvements in the field of geodetic measurements of mantle processes in Antarctica.

Geodetic GNSS measurements to constrain the modelling of ice-induced Earth deformation

Past and recent Antarctic ice-mass changes form the loading and unloading of the Earth's crust. These load changes cause crustal deformations that can be observed by geodetic measurement techniques, especially by GNSS. The response of the solid Earth depends on the timescales of the load and the related rheological properties of the Earth's interior (van der Wal *et al.* 2015; Ivins *et al.* 2020; Barletta *et al.* 2022, this volume). On short timescales (seismic waves), the response is driven primarily by elastic properties; and on

From: Martin, A. P. and van der Wal, W. (eds) 2023. *The Geochemistry and Geophysics of the Antarctic Mantle*. Geological Society, London, Memoirs, **56**, 295–313,
First published online 3 December 2021, https://doi.org/10.1144/M56-2021-22

longer timescales, from decades to thousands of years, anelastic and viscoelastic properties become more important. The ductile behaviour of the lithospheric and upper mantle that is a function of the pressure–temperature distribution, especially in the asthenosphere, govern the response on these longer timescales (Ivins *et al.* 2021, this volume). The slow, time-dependent deformation is known as creep, and dominates the strength of the material below the brittle crust where material strength is determined by the resistance to fracturing. To understand measured crustal deformation and to come up with informed predictions, suitable numerical models have to be set up and their parameters have to be determined. These rheological parameters include the effective elastic thickness of the lithosphere (Burov 2011) and the viscosities of the upper mantle (especially asthenosphere) and lower mantle, respectively, as well as their lateral variations. They can be determined based on seismic-wave tomography and laboratory experiments on material behaviour, but such inferences suffer from a large uncertainty (Ivins *et al.* 2021, this volume). Therefore, constraints on the models are needed.

GNSS observations are used to accurately and consistently determine coordinates and coordinate changes of specially marked points in the bedrock. However, in Antarctica these observations are limited to a few places where bedrock is accessible. It has to be noted that for a long time GPS was the only available system while further satellite navigation systems reached full operation mode and/or civil access (much) later. Today, more systems are available (e.g. GLONASS (Russia), Galileo (Europe) and BeiDou (China)), and modern receivers featuring several hundred receiving channels are capable of recording a multitude of GNSS signals. The resulting coordinate changes, especially vertical velocities or deformation rates, provide independent data at the Earth's surface and, thus, can serve as direct constraints in the modelling.

Short history and types of geodetic GNSS observations in Antarctica

The first, German-led, geodetic GNSS projects started in 1995 in the region of the Antarctic Peninsula and in Dronning Maud Land, East Antarctica (Dietrich 1996, 2000; Dietrich *et al.* 2001, 2004). These measurements formed the nucleus for the Scientific Committee on Antarctic Research (SCAR: https://scar.org/) Epoch Crustal Movement Campaigns, in which many international institutions have since contributed data. The SCAR GNSS database (https://data1.geo.tu-dresden.de/scar) was set-up and is maintained at TU Dresden. In these 'early' GPS years the observations were carried out only as campaign-style or epoch measurements (Figs 1 & 2). One observation epoch could comprise several days of quasi-continuous measurements from which one coordinate solution was computed. Thus, by combining several epochs (observed in different years), coordinate change rates can be estimated. However, it is only possible to deduce linear rates with reasonable accuracy; any non-linear (e.g. seasonal) signals cannot be derived. Similar activities were performed, for example, in the Transantarctic Mountains (1996–2001: Raymond *et al.* 2004; project TAMDEF, first field season 1996–97: Vazquez Becerra 2009), Marie Byrd Land, West Antarctica (1999–2002: Donnellan and Luyendyk 2004) and North Victoria Land (project VLNDEF: Zanutta *et al.* 2017, 2018). Tregoning *et al.* (1999, 2000) started to install continuously operating GPS receivers at Beaver Lake in 1998 and extended the installation in subsequent years to study vertical crustal movement in the region of Lambert Glacier, East Antarctica.

Around the turn of the century, the setting-up of a significant number of permanently recording geodetic GNSS sites was intensified. For this to succeed, the especially challenging task of independent power supply had to be solved. Each permanent site has to be equipped with a large battery pack to provide sufficient electrical charge, together with solar panels and wind generators, for recharging the batteries (Figs 3 & 4). Attempts to use fuel-cell technology were also made in these early years (Tregoning *et al.* 2000). Only in the case of a GNSS site situated near a year-round Antarctic station can a direct power link be utilized, as is the case for the International GNSS Service (IGS: https://www.igs.org) sites SANAE IV, Syowa, McMurdo, Casey, Davis, Mawson, Dumont d'Urville, Palmer, Rothera and O'Higgins (cf. Fig. 5). A significant boost to deploy and run epoch and permanent geodetic GNSS sites in Antarctica was initiated by the International

Fig. 1. Example of a GNSS campaign site: Clark Island, Pine Island Bay, West Antarctica. The GNSS antenna is fixed to the bedrock. Receiver, battery and electronics are stowed in an aluminium box, while the solar panel is used to recharge the battery. Image credits: M. Scheinert.

Fig. 2. Example of a GNSS campaign site: Backer Islands, Pine Island Bay, West Antarctica. Image credits: M. Scheinert.

Polar Year (IPY) 2007–09. The IPY project POLENET was the nucleus for a number of new projects, among which is the USA-led ANET project (Bevis *et al.* 2009; Barletta *et al.* 2018). Here, UNAVCO (University NAVSTAR Consortium: https://www.unavco.org) plays a decisive role in not only providing hardware and engineering expertise for the set-up and maintenance of GNSS sites, but also in operating one of the largest data archives including Antarctic GNSS data. Many national Antarctic programmes have also provided logistic support to carry out these operations in Antarctica.

Reference frame, technique-related issues and accuracy issues

In the data analysis, the linkage of GNSS position measurements to a proper reference system has to be realized (realization of the so-called 'geodetic datum') in order to maintain a practical and accessible solution of the origin, axes and scale of the terrestrial reference frame. In the differential GNSS (DGNSS) method, this is principally fulfilled by the inclusion of reference sites that are IGS sites within Antarctica and at the adjacent continents, and the application of a suitable six- or seven-parameter Helmert transformation. In the precise point positioning (PPP) technique, the role of these fiducial points is taken over by precise ephemeris of the GNSS satellite orbits. For both techniques, and especially in the processing of GNSS data usually spanning time periods of more than 1 year, further data and models, and precise and consistent orbit coordinates as well as clock parameters, have to be introduced: for example, from consistent reprocessing (Rülke *et al.* 2008; Rebischung *et al.* 2016; Villiger and Dach 2020, p. 11). Further parameters introduced into the analysis are phase centre offsets of satellite and receiver

Fig. 3. Example of a GNSS permanent site: Kottas Mountains, western Dronning Maud Land, East Antarctica. The GNSS antenna is installed on the left outcrop (see also Fig. 4). This GNSS site is co-located with a seismometer station of the Alfred Wegener Institute, Germany. On the right outcrop, solar panels and wind generators are mounted. Image credits: E. Buchta.

Fig. 4. Example of a GNSS permanent site: Kottas Mountains, western Dronning Maud Land, East Antarctica (see also Fig. 3). Image credits: E. Buchta.

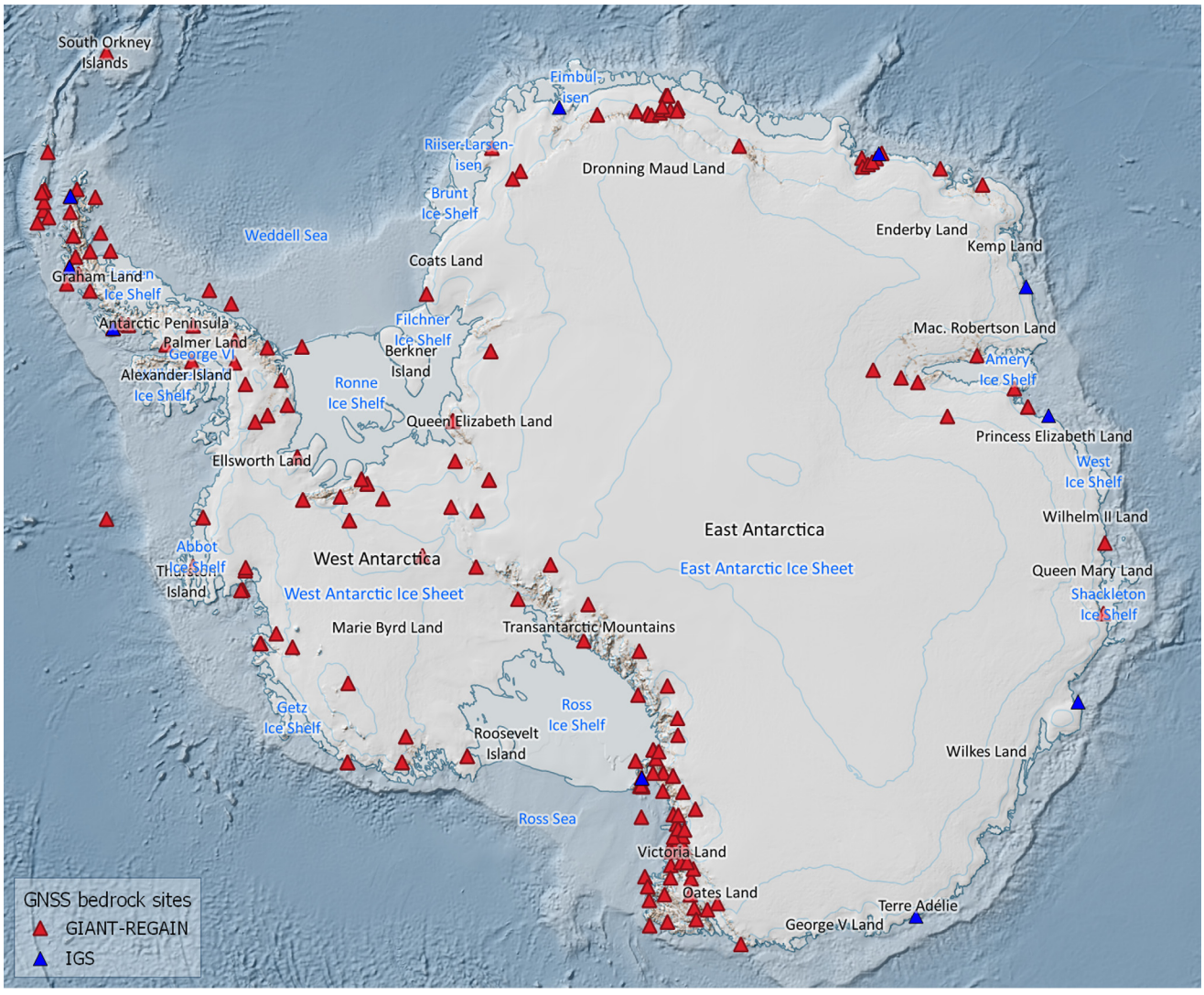

Fig. 5. Distribution of permanent and episodic GNSS sites in Antarctica used in the GIANT-REGAIN reprocessing (red triangles). Blue triangles denote IGS sites.

antennas, and tropospheric and ionospheric signal propagation delay. Geodynamic phenomena are likewise corrected for using models for solid Earth tides, ocean tidal loading and atmospheric loading; see King *et al.* (2010) for a comprehensive overview. In addition, King and Santamaría-Gómez (2016) and Turner *et al.* (2020) emphasize the problem of the separability of the (horizontal) GIA and plate motion from GNSS data. Therefore, GNSS-inferred horizontal velocities have to be used with caution when constraining GIA models in Antarctica.

A particular problem for GNSS in regions of high latitude can be the accumulation of snow on the antenna, which leads to perceived subsidence. In Antarctica, snow was found inside GNSS antennas equipped with radoms (Konfal *et al.* 2016), and the action of blocking the entry of snow led to substantial changes in position time series (Wilson *et al.* 2019). The effect was investigated by Koulali and Clarke (2020), who found that the accumulation of snow depends on local weather conditions and was greatest for cold regions with high wind speed. They showed a substantial effect of snow accumulation on annual signal, but the effect on the estimated trend is not yet known. However, this effect together with the effects of GNSS equipment change or further effects (such as earthquakes) that may prevent an undisturbed time series being obtained have to be taken into account in the estimation of the coordinate velocities. One proven strategy is to mark such events and to estimate the respective velocity only for distinct time periods (where the assumption of linearity is valid). In that respect it has to be emphasized that metadata (such as information on antenna height) are essential. However, often metadata are not, or only incompletely, accessible, which is a further challenge for reliable GNSS analysis.

The recent realization of the (International) Terrestrial Reference Frame (ITRF) is given by ITRF2014 (Altamimi *et al.* 2016), which is based on four basic geodetic space techniques (VLBI (Very Long Baseline Interferometry: see https://vlbi.org), SLR (satellite laser ranging; see https://ilrs.gsfc.nasa.gov), DORIS (Doppler Orbitography and Radiopositioning Integrated by Satellite, see https://ids-doris.org/) and GNSS). If GNSS coordinates and coordinate changes are linked to ITRF2014, they refer to its origin, which is defined as the centre of mass of the entire Earth system (CM). This is true in a long-time sense (or at a secular timescale) since the ITRF2014 origin is tied to the average CM as realized by SLR data (Altamimi *et al.* 2016). Some GIA models refer to CM as well (Spada 2017; Caron *et al.* 2018). However, more often GIA models refer to the centre of mass of the solid Earth (CE) (King *et al.* 2010; Whitehouse 2018). CE experiences a change of its trajectory in the inertial space, while CM is stationary with respect to the inertial system and is, therefore, accessible by orbiting satellites (Blewitt 2003). The effect of the relative velocity of CM with respect to CE on uplift rates has been assessed to be in the range of 0.1 (Thomas *et al.* 2011) to 0.5 mm a^{-1} (Argus *et al.* 2014). Apart from differences in origin definitions used by models and geodetic solutions, different geodetic solutions may refer to different realizations of the CM origin (see the 'Results on mantle-related processes from geodetic data combination' section).

The IGS provides a GNSS-only solution for the ITRF based on the reprocessing of global GNSS reference sites back to 1994, together with orbit ephemerides and further data (Rebischung *et al.* 2016), named the IGS14 reference frame, and which has recently been updated to IGb14. The position accuracy of these GNSS reference sites is on average ±1.5 mm for the horizontal components and ±4 mm for the vertical component (Rebischung *et al.* 2016). The rate of reference frame origin could be determined with an uncertainty of ±0.3 mm a^{-1} from the scatter of the contributing analysis centres (Rebischung *et al.* 2016). This level of uncertainty was confirmed by Riddell *et al.* (2017) when investigating weekly translations of the SLR solutions with respect to the ITRF2014. Adopting a combined power law and white noise model, Riddell *et al.* (2017) concluded that the uncertainty in the rates of SLR X, Y and Z translations is ±0.13, ±0.17 and ±0.33 mm a^{-1}, respectively. This represents an improvement of nearly 30% for the Z component in comparison to the results that Argus (2012) obtained for the previous ITRF2008 solution. Hence, the (long-term) stability of the origin realization was considerably improved in the ITRF2014 solution (Altamimi *et al.* 2016), which provides a decisive precondition for the analysis of GNSS data that may now cover more than 25 years.

To infer coordinate change rates (velocities) for permanent observations methods of time-series analysis can be applied to the daily GNSS position solutions. This allows researchers to adjust simultaneously for different signal parts and noise models. The flexibility of the stochastic modelling is much lower in the case of epoch solutions. The time-series analysis often consists of fitting the coordinate time series with a trajectory model composed of a linear trend, annual and semi-annual signal parts. Thereby, a suitable noise model has to be adopted that usually includes white and coloured (flicker) noise (Williams 2003). Respective software solutions incorporate these noise models (CATS: Williams 2008; HECTOR: Bos *et al.* 2013) and allow a robust trend determination to be performed, even with gaps and jumps in the time series (MIDAS: Blewitt *et al.* 2016). For most sites, coordinate changes can be determined with a precision of ±0.5 mm a^{-1} and better. In terms of accuracy, horizontal velocities can be determined at ±1 mm a^{-1}, while the accuracy of vertical velocities is worse by a factor of 2: that is, at the level of ±2 mm a^{-1} (King *et al.* 2010; Thomas *et al.* 2011; Sasgen *et al.* 2018). The precision may improve with the length of the coordinate time series (King *et al.* 2010). A common mode error (CME) analysis may further improve the precision of the coordinate velocity time series, especially when inferred by PPP, as was shown for the vertical component by Liu *et al.* (2018). CME considers the spatial correlation caused by unmodelled geophysical effects such as atmospheric or non-tidal loading and remaining systematic errors. To investigate the non-Gaussian features of the data, Liu *et al.* (2018) adopted the independent component analysis (ICA), an advancement of the principal component analysis (PCA), taking higher-order non-Gaussian statistics into account. Estimates based on ICA are found to show a stronger correlation with geophysical effects than PCA. After applying spatiotemporal filtering, the mean RMS of the GNSS-observed vertical velocities could be reduced by about 40%, indicating the gain of precision. Likewise, the agreement with predictions of four GIA models could be improved by a mean reduction of 0.9 mm a^{-1} in terms of weighted RMS (Liu *et al.* 2018).

For epoch observations (and, to a certain extent, also for permanent solutions) usually a further uncertainty of 5–10 mm is considered in addition to the precision of daily position solutions to come up with suitable accuracy measures. In this way, residual effects are accounted for: for example, those caused by differences in the site set-up and by uncertainties in the realization of the geodetic datum, especially in the determination of the origin (e.g. Argus *et al.* 2014). The accuracy measures for the resulting trends are inferred by variance propagation (depending on the number of observation epochs and the length of the time span), leading to an accuracy typically of about 4–8 mm a^{-1} for vertical velocities (Rülke *et al.* 2015). However, it could be shown that after a time span of at least 7 years the inferred (linear) rates have similar accuracies, as in the case of continuous observations (Rülke 2009).

Correction for the elastic effect

The GNSS-inferred coordinate change rates reflect the deformation due to instantaneous loading effects and processes governed by the mantle, such as GIA and post-seismic deformation. In order to separate out the mantle contribution, the GNSS-inferred coordinate change rates are commonly corrected for the elastic effect. This starts with the assumption that present-day ice-mass change exerts a load that is immediate or, at least, of comparably short time. Furthermore, it is assumed that at these timescales the response is governed by the elastic properties of the solid Earth. The present-day ice-mass change, for example, is estimated from ice-height observations of satellite altimetry (e.g. ERS-1/2, Envisat ICESat and CryoSat-2: cf. Schröder *et al.* 2019*a*, depending on the time span of the GNSS observations) together with a reasonable assumption on the pattern of firn and ice density (e.g. Groh *et al.* 2012) or applying the mass-budget method based on climate modelling and radar measurements of ice flux across grounding lines (e.g. King *et al.* 2010). In general, the calculation of this elastic effect follows Farrell (1972), where load Love numbers and, subsequently, Green's functions are calculated for a standard 1D Earth model like PREM (preliminary reference Earth model) (Dziewonski and Anderson 1981). Then, the computation can be done in the spectral (i.e. spherical harmonic) domain, while also taking the regional sea-level response into account (e.g. Mitrovica *et al.* 2001). High-resolution computations are necessary, as the measured uplift rates can be sensitive to loading changes from individual glaciers (Barletta *et al.* 2018).

The elastic response might also be sensitive to inhomogeneities in the structure of the lithospheric crust, which are not taken into account in the standard Love number formulation in the 1D Earth model. This sensitivity is pronounced when more localized load signals occur (Dill *et al.* 2015), which is the case for regions of considerable ice-mass loss such as the large outlet glaciers in Amundsen Sea Embayment, West Antarctica, but also for glacial streams in East Antarctica like Jutulstraumen (Dronning Maud Land) or Lambert Glacier, Totten Glacier or Moscow University Glacier (Wilkes Land). Changes in the lithospheric structure might account for variations of up to 25% of the vertical elastic deformation (Dill *et al.* 2015). An open problem is how the elastic and rheological properties can be derived for Antarctica and how they should be taken into account in a consistent way both in the modelling of the instantaneous elastic effect and in the GIA effect. This problem is being approached by further contributions in this Memoir (Ivins *et al.* 2021, this volume; Wiens *et al.* 2021, this volume).

In principle, elastic parameters derived from seismic wave speeds (e.g. Young's modulus and density) are sufficient to calculate elastic effects in surface-loading methods and can be checked by microphysical measurements of lithospheric rocks. Information on elastic properties is usually derived from seismic velocity anomalies. An *et al.* (2015*a*) used about 120 broadband seismographs for calculating a 3D S-velocity model of the Antarctic lithosphere and depth estimates of the Mohorovičić (Moho) discontinuity. From the average ratio between lithospheric mantle and crustal densities, they concluded that the lithospheric mantle is of Archean age. This has also been inferred by isotopic measurements of lithospheric mantle xenoliths (Handler *et al.* 2021, this volume; Martin *et al.* 2021, this volume). The thickest crust is located along the East Antarctic subglacial mountain range (*c.* 60 km in thickness close to Dome A: An *et al.* 2015*a*, figs 1 & 6). Furthermore, in a second paper, An *et al.* (2015*b*) determined the depth of the lithosphere–asthenosphere boundary (LAB). They found East Antarctica to have a 'thick lithosphere similar to other stable cratons' (up to 250 km between Dome A and C) (An *et al.* 2015*b*, p. 8720), while West Antarctic comprises thin crust and lithosphere 'similar to … modern subduction-related rift systems' (An *et al.* 2015*b*, p. 8720). These findings were partially confirmed by Lloyd *et al.* (2020), but were also readjusted to come up with a more detailed picture. In a comprehensive study, Lloyd *et al.* (2020) used adjoint tomography along with data of more than 300 broadband seismometers in Antarctica to image the structure beneath Antarctica, especially the upper mantle and transition zone. In East Antarctica, they found fast shear-wave speed anomalies that mirror 'cold thick lithospheric roots that are characteristic of cratons and Proterozoic fold belts' (Lloyd *et al.* 2020, p. 20). However, thicker lithosphere is suggested only for the interior of East Antarctica, while thinner lithosphere is inferred along the coast, and

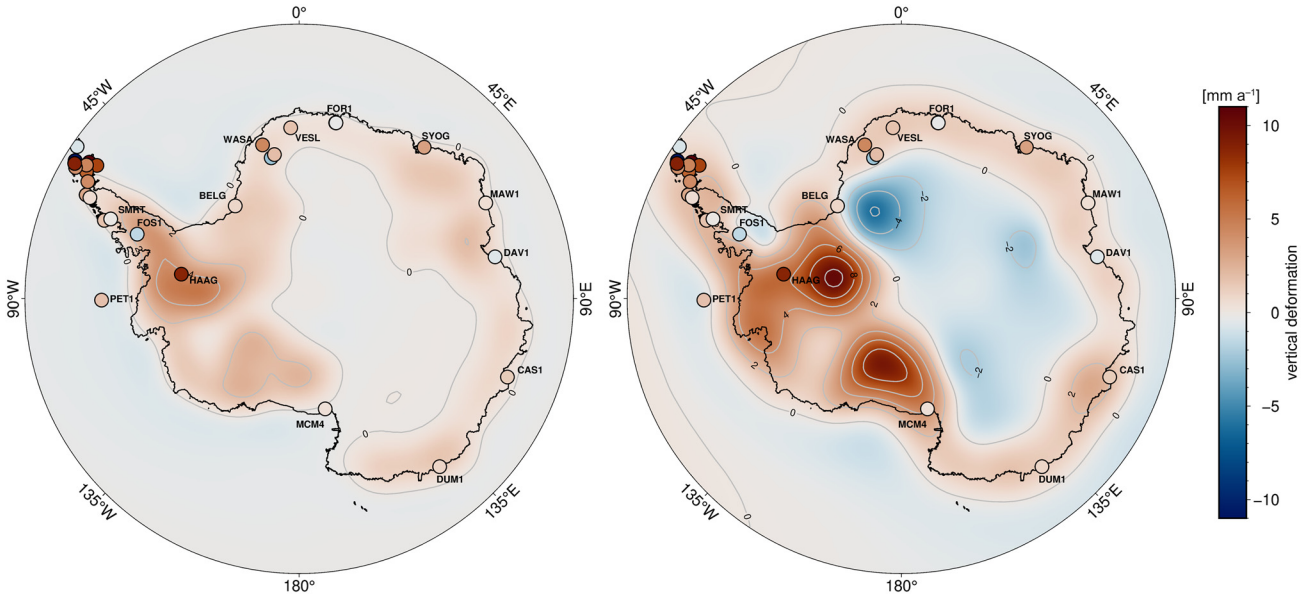

Fig. 6. Vertical deformation rates inferred for selected permanent and campaign GNSS sites in Antarctica (according to Rülke *et al.* 2015, table 1). The GNSS results were corrected for the present-day elastic uplift. In the background, vertical deformation rates are plotted as predicted by respective GIA models: (left) IJ05_R2 (Ivins *et al.* 2013); (right) W12a (Whitehouse *et al.* 2012).

along the sector from western Dronning Maud Land to Enderby and Kemp Land and the Lambert Graben in particular there is a 'much greater variability in lithospheric thickness' (Lloyd *et al.* 2020, p. 20) that may extend for several hundred kilometres inland.

However, many results and hypotheses are still inconsistent or partly contradictory (see Pappa and Ebbing 2021, this volume; Wiens *et al.* 2021, this volume). Gravity data take a more prominent role to estimate crustal thickness and LAB because of the sparse seismic data coverage (Pappa and Ebbing 2021, this volume). Further details on these issues can be found in this Memoir (e.g. Martin *et al.* 2021; Ivins *et al.* 2021; Wiens *et al.* 2021, all this volume). It should be noted that the different methods do not yield the same lithosphere or effective elastic thickness. In seismic studies the LAB is often based on a temperature boundary, whereas for GIA it is based on a transition from elastic to viscous behaviour (e.g. see Nield *et al.* 2018). Steinberger and Becker (2018) concluded that compositional variations in the mantle occur mainly in the upper 150 km. Their model yields lithospheric thickness of up to 250 km for cratons. Effective elastic lithosphere thickness is 'typically about a factor two lower' (Steinberger and Becker 2018, p. 337).

Although it has been argued for a long time that the Antarctic continent is composed of two distinct and contrasting geological provinces (e.g. Adie 1962), it is timely to step back from a uniform picture of one 'East Antarctic unit' (Mieth and Jokat 2014; Jacobs *et al.* 2015; Foley *et al.* 2021, this volume), which is also reflected by the findings of Lloyd *et al.* (2020) (see above).

A further aspect not fully explored yet is the interlinkage between the timescale of the load application and the time-dependent rheological properties of the Earth that govern the deformation response. This is reflected in the following discussion: on the one hand, even at such short timescales as those of semi-diurnal and diurnal Earth tides, effects such as anelasticity are significant and, thus, lead to a deviation from a pure elastic response. Bos *et al.* (2015) explained the discrepancy between GNSS-observed M_2 tidal loading signal and its prediction using ocean tide loading models based on the isotropic PREM (Dziewonski and Anderson 1981) by accounting for the elastic properties of the upper mantle and an anelastic dispersion in the asthenosphere. Bos *et al.* (2015) assumed that dissipation, which is responsible for a reduction in shear modulus, was taking place in an absorption band from seismic up to tidal wavelengths. Ivins *et al.* (2020) emphasized that in the transition from seismic to tidal and even longer wavelengths (up to a typical Maxwell time of *c.* 100 years) deformation has to be explained by taking anelasticity into account and the transition to transient and finally steady-state creep. The latter statement applies, on the other hand, to the problem of timescales for which 'present-day' ice-mass change can be regarded in the elastic framework only. Geodetic GNSS observations in Antarctica cover time periods of more than 25 years (see above), long enough to see the viscous effects due to loading (Nield *et al.* 2014). Ivins *et al.* (2020) discussed how crustal motion induced by glacial loading and unloading on decadal timescales is governed by mantle properties and has to be explained by viscoelastic response.

Thus, it becomes clear that geodetic GNSS observations provide a powerful tool to test rheological properties of the mantle and timescale dependency of the deformation. However, the challenge is to identify those locations on Earth that can serve as a suitable environment for natural experiments. All available processes should be explored such as ocean tidal loading (Bos *et al.* 2015) and body tide deformation (Kang *et al.* 2015) or immediate or catastrophic load changes (e.g. Marderwald *et al.* 2020). One may also focus on regions with fast-retreating glaciers or accelerated mass loss where the elastic response (in the 'classical sense', as described above) makes up more than half of the total observed deformation, as in the case of southern Patagonia (Lange *et al.* 2014) or (parts of) the Greenland ice sheet (Bevis *et al.* 2012, 2019; Nielsen *et al.* 2013). The insights from such experiments have to be transferred to the case of Antarctica in order to investigate their capability to separate and better explain the different effects and timescales of ice-load-driven solid Earth deformation.

Results of geodetic GNSS observations: deformation of the Earth's crust due to GIA

In the framework of the SCAR Epoch Crustal Movement Campaigns Antarctic-wide consistent reanalyses of all data together with IGS data were performed in 2008 and 2015 (Dietrich and Rülke 2008; Rülke *et al.* 2008, 2015). The GNSS-inferred coordinate change rates were corrected for the immediate elastic effect (see the discussion above), and the residual GNSS rates were taken as a ground-truth observation of GIA. However, the residual vertical uplift rates in particular exhibit large differences to the modelled GIA rates according to recent GIA models (Whitehouse *et al.* 2012; Ivins *et al.* 2013) (see Fig. 6). These findings are generally confirmed by investigations by King *et al.* (2010), Argus *et al.* (2011) and Thomas *et al.* (2011). Even if GNSS-inferred deformation rates (especially vertical rates) were used to constrain the modelling of GIA in Antarctica, as in the cases of IJ05_R2 (Ivins *et al.* 2013), ICE6G_C (VM5a) (Argus *et al.* 2014), W12a (Whitehouse *et al.* 2012) and Caron *et al.* (2018), the scatter between the models and the misfit of modelled rates to GNSS-inferred rates are still substantial. Data–model misfit reaches more than 10 mm a^{-1} in the Amundsen Sea Embayment and several millimetres per year in East Antarctica (see also Martín-Español *et al.* 2016*a*), which are comparable to or larger than errors in GNSS-derived trends of 3–4 mm a^{-1} in the Amundsen Sea sector (Martín-Español *et al.* 2016*b*).

Several regional investigations should be highlighted. Bevis *et al.* (2009) presented the first results of the West Antarctic GPS Network (WAGN), which consisted of campaign-style and partly continuous observations. Later, all WAGN sites were upgraded to continuously recording GNSS to form part of the POLENET/ANET project. Bevis *et al.* (2009) found that the GIA models used for comparison over-predicted vertical uplift rates. Zanutta *et al.* (2017, 2018) presented results of a long-term study in North Victoria Land where relatively low uplift rates confirm GIA model predictions but are also subject to tectonic effects. However, the effect of two main tectonic lineaments can only be seen in residual horizontal velocities.

Relatively large uplift rates of more than 10 mm a^{-1} were measured in the Antarctic Peninsula region. Nield *et al.* (2012, 2014) used GNSS data from stations that had mostly been installed since 2009. They carried out viscoelastic modelling to explain the non-linearity in the GNSS time series in the Antarctic Peninsula, and found a combination of elastic and viscoelastic responses fitted the observations. For this, the upper-mantle viscosity had to be constrained to relatively low values (of the order of 10^{18} Pa s). Low viscosity is one of the main findings of the GNSS measurements. However, several questions remain open relating, for example, to the effective elastic thickness of the lithosphere and the range of upper-mantle viscosities (see above). Nield *et al.* (2014) even questioned the validity of (linear) Maxwell rheology (which has been widely used as a standard rheology in GIA modelling). Thus, Nield *et al.* (2018) investigated the impact

of a laterally varying elastic lithospheric thickness in contrast to power-law rheology allowing a viscous lithosphere. Here, the upper-mantle viscosity was not as low as applied by Nield *et al.* (2014). The latter model leads to larger uplift amplitudes and shorter wavelengths, which may be important in better capturing GNSS-inferred deformation that exhibits steeper gradients such as in West Antarctica. Wolstencroft *et al.* (2015) investigated GNSS observations to constrain GIA modelling in the southern Antarctic Peninsula. They localized the largest misfit in the SW Weddell Sea.

The largest uplift rates in Antarctica were measured in the Amundsen Sea sector at the continuously recording ANET sites (Barletta *et al.* 2018), as well as at GNSS epoch sites of TU Dresden (Groh *et al.* 2012, 2014). Including observations of the latest field campaign in early 2017, the TU Dresden group found uplift rates, corrected for the instantaneous elastic effect, of several centimetres per year up to about 4.5 cm a^{-1} (Busch *et al.* 2017). These results are largely underpredicted by the present GIA models. In their regional GIA model refinement, Barletta *et al.* (2018) concluded on a weak shallow upper mantle (from lithospheric base down to 200 km depth) with a viscosity of 4×10^{18} Pa s, a stiffer and deeper upper mantle (200–400 km) of 1.6×10^{19} Pa s, and a transition zone (400–670 km) of 2.5×10^{19} Pa s. To overcome limitations in the Maxwell model, the GNSS-inferred velocities in the Amundsen Sea sector could potentially form useful constraints on viscosity estimates based on seismic anomalies and creep experiments (Ivins *et al.* this volume; Ivins *et al.* 2020, 2021, this volume). Ivins *et al.* (2020) proposed to utilize the extended Burgers model (EBM) in GIA modelling. The EBM might explain rapid uplift even on short timescales such as decades, and enhances GIA uplift predicted by the (classical) Maxwell model by a factor of up to 2.5 (Ivins *et al.* 2020). This attention to shorter timescales has brought to the forefront the largest uncertainty in the modelling, namely the unknown ice history over the last centuries. This problem plays a smaller role in East Antarctica, where viscosity is higher and recent loading does not affect present-day uplift rates as many rates observed in East Antarctica are generally smaller (a few millimetres per year) showing small uplift or even subsidence near the coast. The misfit to GIA model predictions, however, can still be of the same order (Rülke *et al.* 2015) (Fig. 6) at some sites near the coast.

As already stated above (Nield *et al.* 2014), one may investigate non-linear relations between stress and strain rates in contrast to the treatment of the mantle as a Newtonian fluid. This leads to power-law creep equations, where the strain rate varies with time even under constant stress. More important is the fact that mantle viscosity varies with stress (or strain rate). Non-Newtonian flow behaviour has been found to be common in silicate polycrystals even at low stresses but high temperature (Ranalli 1995). However, it is difficult to use GNSS observations to constrain a more realistic (i.e. 3D) mantle rheology together with an ice-history model not starting from an *a priori* (1D) mantle viscosity profile (van der Wal *et al.* 2013). Taking into account the results of laboratory experiments on olivine, the most prominent constituent of the mantle, van der Wal *et al.* (2013) inferred diffusion and dislocation creep flow laws where the latter leads to non-Newtonian flow. However, they stated a difficulty in fitting GNSS uplift rates and sea-level data simultaneously, which may be due to uncertainties in the inferred flow law or not considering mantle minerals other than olivine (van der Wal *et al.* 2013). van der Wal *et al.* (2015) extended this study to the case of Antarctica, acknowledging that seismic studies inferred large viscosity variations in the Antarctic mantle. As applied elsewhere (e.g. Fennoscandia), a finite-element model was extended to also include power-law creep. Global GIA models (ICE-5G: Peltier 2004; W12a: Whitehouse *et al.* 2012) were 'tuned to fit constraints in the northern hemisphere' (van der Wal *et al.* 2015, p. 134) and, thereafter, compared to GNSS uplift rates taken from Argus *et al.* (2014). It could be shown that the models incorporating a 3D Earth structure and composite rheology give smaller misfits between observed and predicted uplift rates, both for W12a and for ICE-5G. Even so, introducing GNSS uplift rates as the only constraints cannot explain to what extent larger variations in the Earth structure beneath Antarctica exist that would certainly increase the influence of 3D rheology (van der Wal *et al.* 2015). However, the impact of modelling 3D rheology leads to variations in mass-balance estimates of the Antarctic ice sheet that are larger than the measurement error.

Thus, improved results can be expected when longer GNSS observation sets become available. The interior of East Antarctica lacks bedrock for realizing GNSS observations; in this case, a combination of measurement techniques may help to constrain GIA models, as will be detailed in the 'Results on mantle-related processes from geodetic data combination' section later in this chapter.

Temporal gravity field variations from satellite gravimetry

Temporal gravity can be measured with terrestrial instruments or with satellites. Although temporal variations have been measured from orbit variations for decades (e.g. Cheng *et al.* 1989), the accurate inter-satellite ranging measurements of the GRACE mission led to a breakthrough in observing mass changes. The GRACE mission is based on inter-satellite microwave ranging, whereby the distance between two satellites that follow each other is measured precisely. The mission operated between 2002 and 2017, and provides a monthly snapshot of the Earth's gravity field (e.g. Tapley *et al.* 2004; Wouters *et al.* 2014). A year after the end of this mission the GRACE-FO mission was launched. The mission aimed for a continuation of the time series, but also carries a novel laser instrument for inter-satellite ranging that has a higher accuracy (Koch *et al.* 2018). The first results showed that the accuracy of the GRACE-FO data was comparable to that of the GRACE data (Landerer *et al.* 2020). However, an accelerometer on one of the satellites had to be switched off, which means that some of the non-gravitational forces cannot be measured accurately. By transferring the accelerations from the leading satellite to the follower, the non-gravitational forces were mitigated. Currently, there is no indication of a bias between the time series of the two missions (Landerer *et al.* 2020), and a time series of mass-balance estimates in Antarctica between both missions appears to be consistent (Velicogna *et al.* 2020).

Three official GRACE science centres currently provide monthly spherical harmonic solutions, so-called level-2 data, with two versions being offered up to maximum spherical harmonic degree and order 60 and degree 96. The spatial resolutions corresponding to a certain maximum spherical harmonic degree L can be approximated by $\pi R_E/L$ where R_E is the mean radius of the Earth. The resolution is limited by the fact that the GRACE and GRACE-FO satellites fly at an altitude of around 500 km, which dampens the gravity signal compared to airborne or terrestrial sensors. The resolution also depends on measurement errors and errors of the applied correction models, which are briefly addressed below. As a result, with the GRACE/GRACE-FO time series one can identify mass-change processes that vary on a timescale of 30 days or more with a spatial resolution of approximately 200–300 km.

Spherical harmonic coefficients of the gravity field form the standard gravity-field products (level-2 data). The satellite gravimetry science product line is set-up in such a way that a user can always undo corrections to go back to an earlier state in the product chain. Important corrections include so-called de-aliasing models for removing temporal gravity signals that originate from non-tidal atmospheric and oceanic mass variations with timescales shorter than the 30 days production scheme. The de-aliasing products are based on a numerical weather prediction model and ocean bottom pressure output from a global ocean circulation model (Dobslaw *et al.* 2017). Uncertainties in the de-aliasing models still contribute a significant part of the GRACE measurement error (Kvas and Mayer-Gürr 2019). GRACE/GRACE FO measurements of very-long-wavelength signals are less accurate. Therefore, the C_{20} coefficient is usually replaced by a solution from satellite laser ranging (Dahle 2020). The same holds for the C_{30} coefficient, which also influences the Antarctic mass balance (Loomis *et al.* 2019; Velicogna *et al.* 2020).

The error in the GRACE data comprises sensor errors and errors of the correction models. Because of the sampling of the GRACE mission along a polar ground track, these form a characteristic pattern of north–south-orientated bands or stripes (Swenson and Wahr 2006). Because of undersampling of the high-frequency geophysical signal, errors in the correction models end up in the Earth's flattening term (C_{20}) and other low degree and order terms, but also spherical harmonic order around 15 and multiples thereof. This finally results in the equivalent water-height product being affected by aliasing with periods of 100 days up to several years (Seo *et al.* 2008). Part of the north–south-orientated errors can also be understood as the interaction of the shifting ground-track pattern with the low-frequency quasi-periodic gravitational signal (Peidou and Pagiatakis 2020).

As a result of this complex interplay of measurement errors, correction models and sampling, it has proven difficult to provide an accurate statistical description of the errors. The north–south error signal is a result of correlation in the data, but off-diagonal terms in the full covariance matrices did not provide corresponding information (Wahr *et al.* 2006). Therefore, most studies used the standard deviation of least-squares residuals as a proxy for the error (e.g. Chen *et al.* 2006; Velicogna and Wahr 2006). However, autocorrelation can result in an underestimation of the error by a factor of 2 or more (Horwath and Dietrich 2009; Williams *et al.* 2014). Because of the errors mentioned above, filtering is generally applied. Filters follow different approaches: (i) smoothing the short-wavelength with weights derived from a Gaussian function (e.g. Velicogna and Wahr 2006); (ii) applying an anisotropic filter such as by Kusche *et al.* (2009); (iii) applying statistical tests to spherical harmonic coefficients (Sasgen *et al.* 2007); or (iv) separating signals by empirical orthogonal function analysis (King *et al.* 2012). Because the exact noise properties are unknown, it is difficult to optimize the filter settings. However, the GIA signal is mostly linear across the measurement period, which means that the strength of the signal increases in an estimation of the trend. Less additional filtering is necessary as a result, with recent studies using a 250 km half-width of the filter (Velicogna *et al.* 2020), which results in higher-resolution mass-change estimates (Velicogna *et al.* 2020), whereas earlier results used a half-width of 800 km (Chen *et al.* 2006). This also reflects improvements in the background model corrections that reduce the noise at smaller spatial wavelengths.

An improvement in resolution was also demonstrated by using data from the GOCE (Gravity field and steady-state Ocean Circulation Explorer) satellite mission. This satellite carried a gradiometer that accurately measures the accelerations between proof masses levitating inside the satellite. The mission was designed for accurate measurement of the static gravity field. Its measurements were not very sensitive to gravity changes in the spatial scale of the ice-mass change. Combined with a relatively short lifetime of 3 years, GOCE was not expected to contribute to time-variable gravity estimates. However, a combination of GOCE and GRACE improved the spatial resolution of the mass changes in the Amundsen Sea sector (Bouman *et al.* 2014). Further improvement in resolution is possible by terrestrial gravity measurements. Terrestrial measurements of time-variable gravity can observe solid-Earth processes such as volcano inflation, solid Earth tides, slow slip events, GIA or co- and post-seismic signals (Van Camp *et al.* 2017). Instruments can be divided into absolute gravimeters that measure the absolute value of gravity and relative gravimeters that measure gravity differences with respect to a reference point or acquire time series. In Antarctica, absolute measurements were realized at several sites (Mäkinen *et al.* 2007). The measurements are sensitive to the uplift resulting from GIA, but the analysis of 5 years of data acquired at Syowa showed that the GIA signal is still obscured by changes in atmospheric mass and snow changes (Aoyama *et al.* 2016). Therefore, observations of solid Earth mass changes in Antarctica mostly rely on data from the GRACE and GRACE-FO mission.

Spherical harmonic coefficient sets provided by the GRACE data-processing centres can be synthesized to produce gravity changes on a map, or can be transformed to changes in equivalent water-layer thickness, which assumes that all gravity change originates from a layer of water at the Earth's surface. Water-layer-thickness changes are also provided by GRACE processing centres and other institutes as so-called level-3 products. Mascons provide an alternative to spherical harmonic solutions, which are based on regional mass concentrations obtained from a direct inversion of the inter-satellite distances for predefined regions on the Earth (Loomis *et al.* 2019). The mascon technique can also be applied to the spherical harmonic coefficients. This is documented, for instance, by Schrama *et al.* (2014), where it is used to obtain ice-mass-change estimates for basins in Antarctica. Leakage forms one of the potential error sources in surface-mass-change estimates, based either on synthesized equivalent water-layer grids or on mascons. Leakage refers to errors in the spatial attribution of mass changes associated with observed gravity field changes (Swenson and Wahr 2002; Horwath and Dietrich 2009). Different strategies for mitigating or correcting leakage effects have been developed based on *a priori* information on the signal location, patterns or covariance (e.g. King *et al.* 2012; Landerer and Swenson 2012; Harig and Simons 2015). Mascon approaches particularly lend themselves to incorporating such information (Wiese *et al.* 2016; Loomis *et al.* 2019).

Most of the global signals in GRACE level-2 data originate from changes in water storage. However, solid Earth signals are also visible, the main ones being GIA (e.g. Tamisiea *et al.* 2007), co-seismic signals and post-seismic signals (e.g. Chen *et al.* 2007; Han *et al.* 2016). Time-variable gravity from other mantle-flow processes is currently at the edge of detection of the GRACE mission (Ghelichkhan *et al.* 2018). In large parts of Antarctica, the increasing gravity signal is dominantly due to GIA. Post-seismic relaxation could potentially form a significant signal if it is also detected in GNSS data (King and Santamaría-Gómez 2016; Barletta *et al.* 2022, this volume). Ice-mass changes form a loading effect to which the solid Earth responds, but this can be taken into account by elastic effect only as described in the 'Geodetic GNSS measurements to constrain the modelling of ice-induced Earth deformation' section. Because the gravitational effect due to deformation is much smaller than the mass change itself, the elastic effect is also smaller than in GNSS uplift rates. It can be satisfactorily modelled by using Green

functions based on a reference Earth model (see the section on 'Geodetic GNSS measurements to constrain the modelling of ice-induced Earth deformation').

The difficulty in interpreting gravity data is that it also contains other signals, so that corrections are required to be able to discern the signals of interest, even after the de-aliasing models. In Antarctica, the main signal of interest is the ice-mass loss in West Antarctica and parts of East Antarctica. Therefore, the solid Earth signal due to GIA is corrected for by subtracting gravity changes predicted from numerical models from the GRACE data (e.g. Velicogna and Wahr 2006; Ivins *et al.* 2013; Sasgen *et al.* 2013). An ensemble of forward GIA models was used to quantify uncertainty yielding error bars larger than the signal (Barletta *et al.* 2008). More realistic estimates can be obtained by using constraints on the GIA process in Antarctica such as ice margins and sea-level data in a Bayesian approach (Caron *et al.* 2018). This yields standard deviations of 10 mm a^{-1} water equivalent in large parts of West Antarctica and coastal areas in East Antarctica, compared to a maximum signal in West Antarctica of 160 mm a^{-1} (Ivins *et al.* 2013). It is important to realize that both GIA and satellite gravimetry are global in nature, and GIA outside Antarctica contributes to the mass changes signal within Antarctica. This effect is estimated to be between 17 and 42 Gt a^{-1} (Caron and Ivins 2020), which is significant compared to 160 Gt a^{-1} attributed to ice-mass loss over the period 1992–2017 (Shepherd *et al.* 2018).

Another approach to address signal separation is to combine GRACE data with complementary data, as will be discussed in the next section. Furthermore, a separation in the time domain is possible. The GIA signal is linear over the timescale of the GRACE mission; therefore, the acceleration signal will not be affected by the GIA (Velicogna 2009). An exception may be seen in areas where the viscosity is so low that the GIA process can contribute to an acceleration over a short time period (Barletta *et al.* 2022, this volume).

The Ice Sheet Mass Balance Inter-comparison Exercise (IMBIE) is aimed at summarizing the ice-sheet mass balance for Greenland and Antarctica (Shepherd *et al.* 2018, 2020). In both papers the GIA signal is reduced from observations using GIA models. As noted before, the uncertainty in the GIA correction is significant, and depends on the knowledge of past ice thickness and rheology. The largest uncertainty is due to the unknown ice thickness. This is reflected in the results presented by, for instance, Schrama *et al.* (2014), who discussed mass changes for the Antarctic ice sheet between 2003 and 2013 based on GIA models adopting different ice histories. They found the Antarctic ice-mass balance using GIA models (at this time new) IJ05_R2 (Ivins *et al.* 2013) and W12a (Whitehouse *et al.* 2012) to be half that inferred using the ICE-5G-based models (Peltier 2004).

Figure 7 (see also Shepherd *et al.* 2018) shows the mass change of the Antarctic ice sheet including subdomains based on a number of techniques including spaceborne gravimetry. The gravimetric estimates are in turn based on a variety of contributions to IMBIE where different processing approaches were applied based on the options mentioned above. It was found that the total melt of land ice between 1992 and 2017 contributed 7.6 ± 3.9 mm to sea-level rise. The GIA correction in East Antarctica suffers from a poor availability of constraints. In other regions, the high uplift rates observed by GNSS are not captured in the GIA models used in the IMBIE study, as these did not include ice-thickness changes more recent than the last few hundred years. An improvement on the latter aspect is the use of GIA models, which represent the regional properties of the solid Earth (e.g. Barletta *et al.* 2018). However, information on last millennial ice-sheet thickness necessary for such modelling is not available continent-wide. Models that consider variations in viscosity already exist (Geruo A. *et al.* 2013; van der Wal *et al.* 2015; Gomez *et al.* 2018), but the uncertainty in viscosity derived from seismic information is still large (Ivins *et al.* 2021, this volume).

Results on mantle-related processes from a combination of geodetic data

Traditionally, GIA is modelled using two key inputs: ice-loading history; and a model of solid Earth properties and structure (Barletta *et al.* 2022, this volume). GIA rates modelled in this way are called forward-modelled GIA. An alternative way to derive GIA is through combining different geodetic observational techniques, such as gravimetry ('Temporal gravity field variations from satellite gravimetry' section), altimetry and/or GNSS displacements (sse the introduction). In Antarctica, the satellite gravity missions GRACE and GRACE-FO observe a superposition of signals mostly originating from two different sources: mass variations within the surface layer; and GIA-induced mass variations ('Temporal gravity field variations from satellite gravimetry' section). The surface layer contains variations of ice and

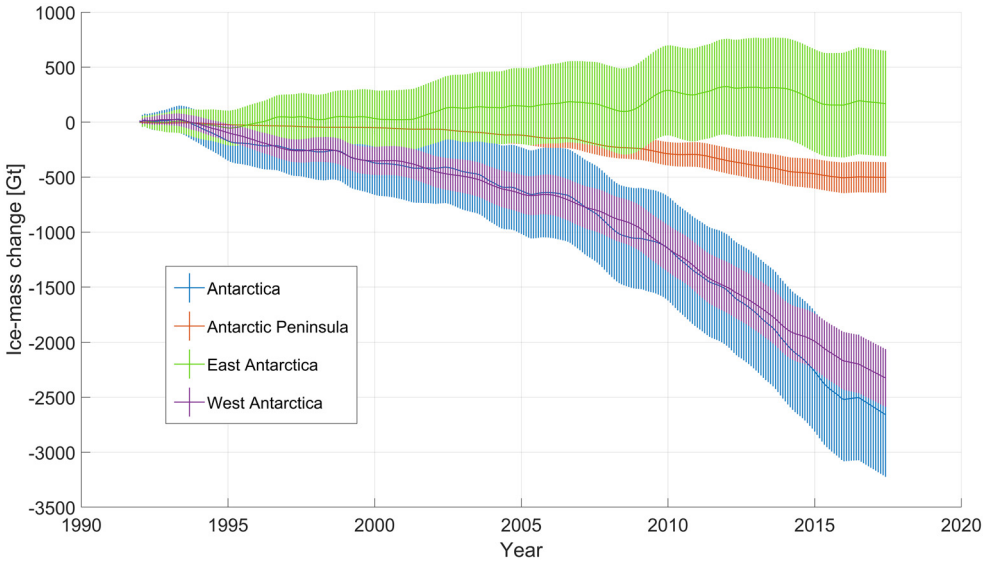

Fig. 7. Cumulative mass change of the Antarctic ice sheet, separated in West and East Antarctica, Antarctic Peninsula and the entire ice sheet, including 1σ error bars (unit: Gigaton). The figure is based on the data published by Shepherd *et al.* (2018) and https://www.imbie.org (last accessed: 8 September 2021), and corresponds to Shepherd *et al.* (2018, fig. 2).

firn, whereby the term 'firn' is used to describe all associated processes such as snowfall, melt and firn compaction (Ligtenberg *et al.* 2011). The variations within the surface layer will usually be and hereafter termed 'ice-mass changes'. GRACE and GRACE-FO have a different sensitivity to ice-mass changes than to GIA-induced mass changes due to the large differences of the corresponding densities ('Geodetic GNSS measurements to constrain the modelling of ice-induced Earth deformation' section).

In contrast to *mass* changes measured by gravimetry missions, altimeters track *height* changes at high spatial resolution. Height changes associated with surface processes are typically much larger than those caused by GIA. Thus, they are more easily detectable by altimeters due to a better signal/noise ratio. However, the altimetry signal contains the height changes related to both GIA and surface processes.

Dedicated ice radar satellite altimetry missions include Envisat (2002–12) or CryoSat-2 (2010–), and the laser altimetry missions ICESat (2003–09) and ICESat-2 (2018–). Radar altimeters provide the longest observational record of these two types. They are not sensitive to clouds (as is the case for laser altimeters) and, therefore, can measure under all atmospheric conditions. However, they have difficulties in regions of large surface slopes (Brenner *et al.* 2007). Furthermore, since the radar signal penetrates snow, an accurate model for surface penetration is required. When converting altimetry height changes into mass changes, both radar and laser altimetry data should be first corrected for firn compaction because the corresponding height changes are not associated with a mass change. In addition, this conversion requires assumptions about the density of snow and ice, which represents the largest source of uncertainty when using altimetry data for deriving mass changes. The processing of input data for a regional inversion of geodetic observations in Antarctica is discussed in detail in Sasgen *et al.* (2018). In the summer of 2020, a so-called CryoSat-2/ICESat-2 (CRYO2ICE) resonance campaign took place to improve the accuracy of ice-sheet elevation time series, in which both satellites are almost simultaneously passing the same areas providing, for the first time, radar and laser measurements of the same geophysical condition (https://earth.esa.int/eogateway/missions/cryosat/cryo2ice).

As discussed in the 'Geodetic GNSS measurements to constrain the modelling of ice-induced Earth deformation' section, GNSS observations represent a valuable constraint on GIA. However, they need to be corrected for elastic deformation (see 'Geodetic GNSS measurements to constrain the modelling of ice-induced Earth deformation'). Thus, for the computation of the elastic signal, an accurate knowledge of ice-mass changes with high spatial and temporal resolution is required. In addition, when using GNSS to constrain GIA, one has to keep in mind the fact that GNSS-inferred site velocities usually refer to CM (see the subsection 'Reference frame, technique-related issues and accuracy issues') and, therefore, contain global GIA. This means that the GNSS signal over the Antarctic ice sheet contains: (i) Antarctic GIA; (ii) Antarctic elastic deformation; and (iii) long-wavelength signal from non-Antarctic sources, which are mostly driven by GIA in the northern hemisphere (Caron and Ivins 2020).

The GIA-derived rates based on observations are labelled 'empirical' to guarantee a clear separation from the forward-modelled GIA rates. Sometimes, empirically derived GIA rates are also called 'inverse' (Martín-Español *et al.* 2016*a*). The methods developed to assess Antarctic GIA can be arranged in four categories:

1. Forward modelling of GIA based on ice-load history and assumed properties and structure of the solid Earth (e.g. Peltier 2004; Ivins and James 2005).
2. Forward modelling of GIA while constraining it using geodetic observations such as GNSS (e.g. Nield *et al.* 2014, 2016; Barletta *et al.* 2018) or GRACE and GPS (Sasgen *et al.* 2013).
3. Estimating GIA empirically using complementary geodetic observations while constraining it using forward models. For this, Schoen *et al.* (2015), Zammit-Mangion *et al.* (2015) and Martín-Español *et al.* (2016*b*) used a hierarchical Bayesian framework. Sasgen *et al.* (2017) extended their approach by including local viscoelastic response functions (Barletta *et al.* 2022, this volume) to account for lateral variations in the Earth structure.
4. Estimating empirical GIA from complementary geodetic observations independent of *a priori* assumptions about the Earth's viscosity structure and ice-loading history (e.g. Riva *et al.* 2009; Gunter *et al.* 2014; Engels *et al.* 2018; Willen *et al.* 2020).

Independence is a very important aspect as it allows forward-modelled and empirically derived GIA to be validated, providing insights into the underlying geophysics. Therefore, in this section, the main emphasis will be put on the fourth category. The first and second categories are discussed in the chapter by (Barletta *et al.* 2022, this volume). It is important to mention here that GIA encompasses a range of observables including solid Earth deformation and deformation of the shape of the geoid. In the following, unless stated otherwise, the rates of surface deformation associated with GIA will be discussed.

The concept of deriving the *empirical* GIA was first introduced by Wahr *et al.* (2000). Prior to the launch of the GRACE and ICESat satellite missions, Wahr *et al.* (2000) suggested a combined approach based on simulated altimetry and gravimetry data to simultaneously solve for GIA and ice-mass changes. Velicogna and Wahr (2002) extended this approach by additionally considering simulated continuous GNSS observations to account for time-varying density within the surface layer. However, the first real data implementation was performed by Riva *et al.* (2009) for the whole Antarctic ice sheet based on 5 years of ICESat and GRACE data. Their results demonstrated that GIA (Fig. 8a) and surface processes could indeed be separated by combining the two complementary geodetic observations.

Following Riva *et al.* (2009), Groh *et al.* (2012) focused their research on the Amundsen Sea sector in West Antarctica for which they derived GIA and ice-mass changes for the 6 year observation period utilizing GRACE and ICESat observations. Their results suggested a strong viscoelastic uplift confirmed (at that time) by only two seasonal GNSS campaigns at three sites located in this region.

In the time since the work by Riva *et al.* (2009), additional data from a regional atmospheric climate model (RACMO) were made available to the scientific community. Two products of the RACMO are usually utilized: the firn densification model (FDM: Ligtenberg *et al.* 2011) and the surface mass balance (SMB: Lenaerts *et al.* 2012), which describe temporal processes within the firn layer in terms of height and mass changes, respectively. Both the SMB and FDM temporal variations are inherently linked. To improve the methodology of Riva *et al.* (2009), Gunter *et al.* (2014) incorporated the information provided by RACMO into the gravimetry/altimetry combination approach. After establishing a calibration approach of the empirically estimated results to a low-precipitation zone in East Antarctica, their derived GIA consistently outperformed forward-modelled results when compared to GNSS displacements, as was shown by Gunter *et al.* (2014) and Wolstencroft *et al.* (2015). Moreover, the high GIA uplift rates in the Amundsen Sea sector that were first suggested by Groh *et al.* (2012) could be confirmed and its spatial pattern could be demonstrated (Fig. 8b). Gunter

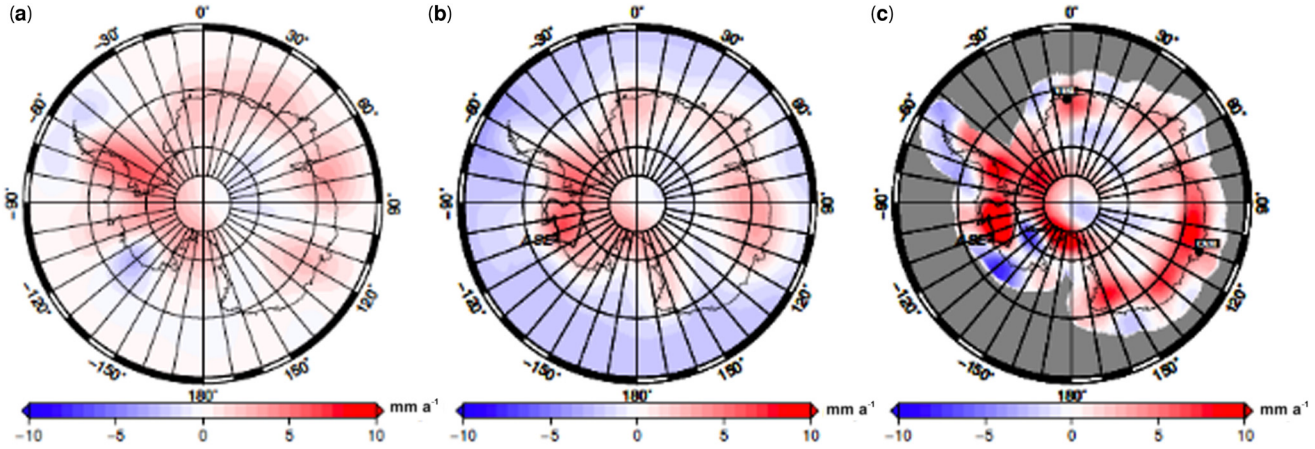

Fig. 8. GIA derived from: (**a**) Riva *et al.* (2009) using the gravimetry–altimetry combination approach; (**b**) Gunter *et al.* (2014), who additionally incorporated variations within the firn layer using climate data from RACMO and found strong uplift in the Amundsen Sea sector; and (**c**) Engels *et al.* (2018), who improved the combination approach to achieve high spatial resolution of the estimated signals.

et al. (2014) suggested that the disagreement between forward-modelled and empirically derived GIA rates in this region could be caused by the fact that the forward GIA models do not typically consider ice-load changes over the last 1000 years, which may, however, be a significant signal.

After allowing the spatial GIA length scale to vary from 500 km over West Antarctica and linearly increasing up to 1700 km over East Antarctica, as opposed to using a fixed GIA length scale by Schoen *et al.* (2015), Martín-Español *et al.* (2016*b*) also derived a strong GIA signal in the Amundsen Sea sector. Considering the weak Earth structure in the determination of utilized viscoelastic response functions, Sasgen *et al.* (2017) concluded that the large uplift in the Amundsen Sea sector is likely to have been caused by a rapid viscoelastic response to more recent ice retreat and thinning. A statistically significant purely data-driven strong GIA uplift was also retrieved by Engels *et al.* (2018). They suggested an approach that simultaneously (i) removes the correlated noise in gravity data (see the 'Geodetic GNSS measurements to constrain the modelling of ice-induced Earth deformation' section) and (ii) consistently combines them with high-resolution data from the altimetry–RACMO combination, yielding high spatial resolution of the empirically estimated GIA (Fig. 8c) and ice-mass change signals.

Empirical GIA models for Antarctica do not contain all long-wavelength signals from GIA or loading outside Antarctica. Global inversions can provide useful constraints providing a robust long-wavelength GIA signal as well as a regional GIA signal, albeit with lower accuracy. Such global inversion requires additional constraints. Over the ocean, researchers use ocean bottom pressure from ocean models (e.g. Wu *et al.* 2010) or sea-level observations from radar altimetry (Rietbroek *et al.* 2016) as additional input. Recently Jiang *et al.* (2021) obtained a global inverse GIA model with a rate of change of C_{20} that matched that of the GIA models and estimates from satellite laser ranging, while at the same time showing the enhanced GIA signal in areas of low viscosity such as the Amundsen Sea sector.

Recent GIA models that consider late Holocene ice-mass changes support the large GIA-induced uplift in the Amundsen Sea sector, which is known for its relatively thin lithosphere and low mantle viscosity (Nield *et al.* 2016; Barletta *et al.* 2018; Gomez *et al.* 2018). According to Barletta *et al.* (2018), who used GNSS observations to constrain mantle viscosity, the forward-modelled GIA-induced mass changes over that region for the GRACE time period range between 13.5 and 19.4 Gt a^{-1}. The empirical estimate by Engels *et al.* (2018) of 17.8 ± 0.7 Gt a^{-1}, which is completely independent of GNSS uplift rates used by Barletta *et al.* (2018), compares very well with the forward-modelled GIA. It is remarkable that empirically estimated and forward-modelled GIA solutions start to converge in this region, which is very important in light of current discussions regarding the stability of the Antarctic ice sheet and its contribution to sea-level rise (Engels *et al.* 2018; Larour *et al.* 2019).

The low mantle viscosity over the Amundsen Sea sector not only yields a localized GIA signal but also shortens the GIA response timescale from a century to decades. The GIA response is even predicted to accelerate with time, potentially preventing the complete collapse of the West Antarctic ice sheet (Barletta *et al.* 2018). The high empirical and forward-modelled GIA uplift rates in the Amundsen Sea sector provide arguments for a much more dynamic Antarctic ice sheet and, thus, questioning the assumption of a linear GIA signal that has been made in all earlier studies. Evidence of a time-variable GIA trend is also found in regions outside Antarctica, for instance when analysing geodetic observations in SE Alaska from 1992 to 2012 (Hu and Freymueller 2019). However, the open question is whether the non-linear GIA signal modelled by Barletta *et al.* (2018) in West Antarctica can be verified over a time period longer than a decade using a purely data-driven approach. For this, Willen *et al.* (2020) have undertaken a first attempt towards deriving monthly GIA-induced mass changes.

Summary and future research directions

Accurate geodetic data can constrain the uplift rate and the mass-change rate from mantle processes in Antarctica. Despite the logistical difficulty, GNSS observations have been collected since the 1990s. Satellite techniques provide the largest share of observations because they cover the entire continent apart from a small cap around the South Pole due to the inclination of the respective missions. Radar altimetry comprises the longest time period of the geodetic missions. However, altimetric height changes mainly reflect the change in ice thickness, while the GIA component in the height change is at least one order of magnitude smaller. Therefore, this chapter focused on GNSS and satellite gravimetry. However, altimetry plays an important role in untangling the ice-mass change signal in satellite gravimetry, and empirical GIA models can

be seen as an independent product that can constrain the modelling of GIA.

GNSS measurements were started by campaigns, but more and more commonly continuous GNSS stations have been put into place since the turn of the century, especially since the IPY (2007–09). The remote environment necessitated installing independent power supplies from solar and wind generators, and protection from weather conditions. Standard GNSS processing methodology is followed, such as aligning the solutions to the terrestrial references by including IGS reference stations from adjacent continents. The accuracy achieved for horizontal velocities is typically 1 mm a^{-1}, while the accuracy of the vertical velocity is at the level of 2 mm a^{-1} (King *et al.* 2010; Thomas *et al.* 2011; Sasgen *et al.* 2018). This accuracy is sufficient to observe the solid Earth signal in many regions of Antarctica, although non-linear motion can often be better characterized than linear motion. However, identifying the viscous signals requires knowledge of the elastic loading, which becomes the largest error source when using GNSS to constrain GIA models. Still, GNSS provides the only constraint in large parts of Antarctica. The large uplift rates observed in the Antarctic Peninsula and the Amundsen Sea Embayment have motivated an increased effort to model GIA in low-viscosity regions. Similar to studies in Alaska, Iceland and Patagonia, it is now clear that parts of West Antarctica and the Antarctic Peninsula must be underlain by a low-viscous mantle. This is an important constraint on 3D viscosity maps that are created from seismic models (Ivins *et al.* 2021, this volume).

In order to come up with a consistent and homogeneous solution for coordinates and coordinate changes of bedrock sites in Antarctica, the GIANT-REGAIN (Geodynamics In ANTarctica based on REprocessing GNSS DAta INitiative) project compiles the most complete dataset of geodetic GNSS measurements recorded at bedrock sites in Antarctica. First results of this processing can be expected in 2022.

The success of improving constraints on the solid Earth response depends on the *continuation* of geodetic GNSS observations in Antarctica in order to extend the time span, as well as on the realization of *continuous* measurements in order to detect annual and non-linear signals. Observing the uplift over a longer time period will provide vital constraints to improve understanding of the evolution of the Antarctic ice sheet and its interaction with the solid Earth. Other research topics that can be addressed with longer time series are the importance of anelastic behaviour for timescales beyond instantaneous loading. Longer time series also help to reduce the error in horizontal velocities and to better separate the plate motion signal. The GIA signal in horizontal velocities is much smaller than in vertical uplift rates, but they are more sensitive to viscosity and possibly a viscosity contrast (Hermans *et al.* 2018). The analysis of horizontal velocities near the Ross Sea demonstrated the potential for constraining the viscosity contrast across that region (Konfal *et al.* 2018).

Satellite gravimetry using GRACE and GRACE-FO provides mass-change measurements with a temporal resolution of 1 month and a spatial resolution of around 300 km. With ground tracks passing near the poles, the coverage of

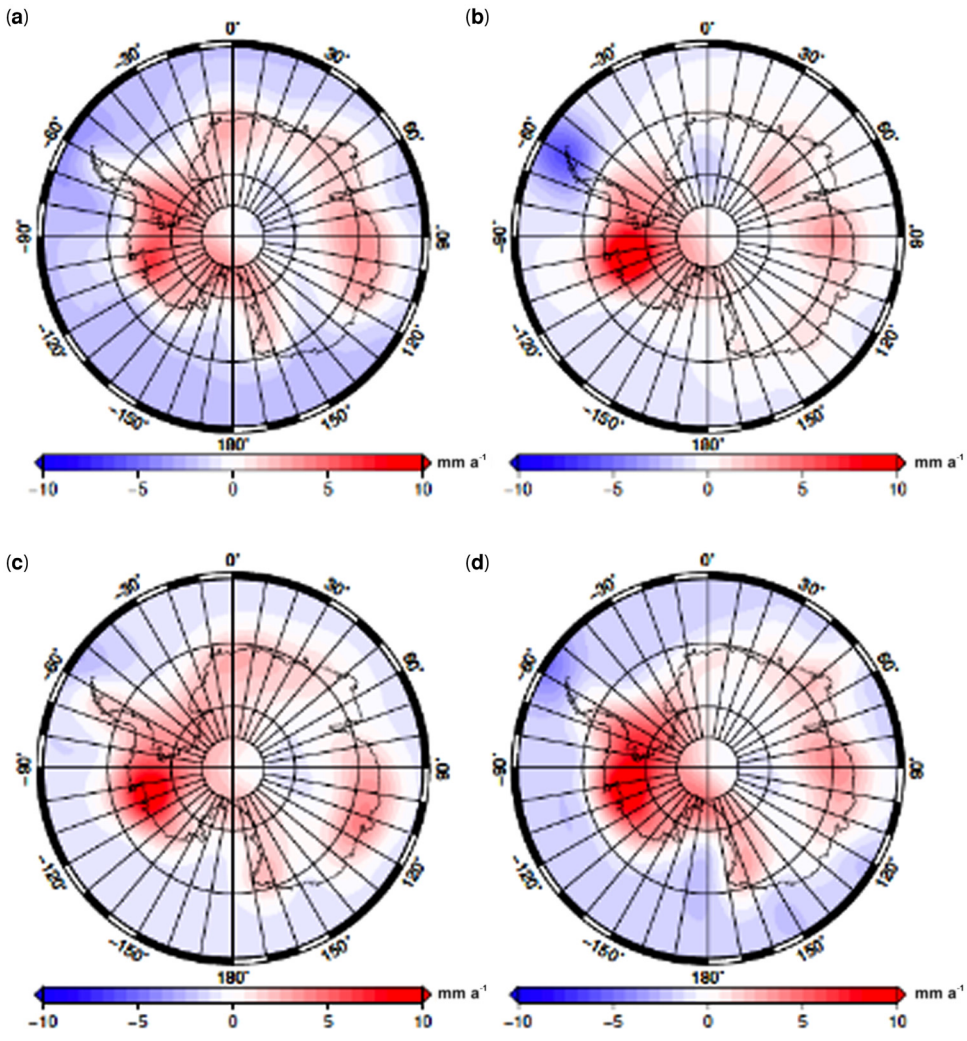

Fig. 9. (**a**) GIA estimated by Gunter *et al.* (2014). GIA estimated over the same time span and applying exactly the same methodology as Gunter *et al.* (2014), but using a new dataset for (**b**) satellite altimetry (publicly available: cf. Schröder *et al.* 2019*b*); (**c**) RACMO2.3p2 (provided by M. van den Broeke and P. Kuipers Munneke, Utrecht University, The Netherlands); and (**d**) satellite gravimetry (publicly available: cf. Mayer-Gürr *et al.* 2018).

Antarctica is much better than that of low-latitude regions. However, corrections models (e.g. for atmospheric pressure) can be less accurate in Antarctica and correlated errors manifesting as north–south stripes are still present. As for GNSS, the signal separation between current ice-mass changes and the readjustment to past mass changes remains the greatest problem. It is usually the ice-mass changes that are the focus of interest. However, satellite gravimetry needs to be corrected for GIA in order to obtain the real ice-mass changes, with this effect being the greatest source of noise in trend estimates. This demonstrates the importance of improved realism and accuracy in numerical GIA models taking into account lateral and temporal changes in viscosity, for example, and extending ice melt further back in time. The consistency between mass changes derived from satellite gravimetry as well as from radar altimetry or input–output mass changes provides a validation of GIA models. However, the problem of uncertainty in GIA predictions can only be solved by including further datasets. Apart from the empirical GIA modelling based on geodetic data, constraints on the GIA process (e.g. in the form of ice-margin data, measurements on bedrock and relative sea-level curves) are crucial.

For deriving empirical GIA estimates, the quality and properties of the input datasets are pivotal to the combination methodology. Following the approach introduced by Gunter *et al.* (2014) in their sensitivity study of Antarctic GIA, Willen *et al.* (2020) concluded that the estimated GIA is strongly sensitive to input datasets (as can be expected for a combination of real data). The sensitivity of the estimated GIA to different datasets is clearly visible in Figure 9 (reproduced from Willen *et al.* 2020). Apart from the data themselves, the input includes assumptions on the density of snow, ice and the upper mantle. Although several attempts have been made to improve the combination approach, a thorough validation of all datasets involved is still missing. Especially in light of large interannual variations in the Antarctic climate (Ligtenberg *et al.* 2012) and the possible non-linearity in the GIA signal (Barletta *et al.* 2018), a sophisticated approach for time-series analysis, such as suggested by Engels (2020), could be used to analyse and validate temporal variations of all input data prior to combining them: (i) to improve our understanding of the evolution of Antarctic geophysical processes; (ii) to identify significant disagreements; and (iii) to adjust the uncertainties correspondingly, which is crucial when combining data from different observational techniques.

Extended time series yielded by satellite gravimetry (GRACE-FO), altimetry (ICESat-2) and GNSS, along with improved methodologies, will increase the spatiotemporal resolution and the reliability of empirically derived GIA. Moreover, data-driven GIA should be extensively compared against independent GIA models that consider ice-mass changes in the late Holocene in addition to the last glacial maximum, as well as a wide range of plausible Earth parameters based on seismic, gravity and petrological information. Only a close collaboration of modellers, geoscientists and remote-sensing experts can help to increase the accuracy of the derived GIA models, which are so crucial in quantifying Antarctic ice-mass loss and in predicting feedback effects on future changes to ice dynamics.

Acknowledgements The successful realization of *in-situ* measurements in Antarctica is always a result of a collaborative effort of many people both in science and logistics as well as of many nations. Therefore, we would like to acknowledge the fruitful and constructive co-operation with all colleagues who supported field work and were involved in the research in Antarctic geosciences. Especially we would like to emphasize the collaboration within the Scientific Committee on Antarctic Research Expert Group on 'Geodetic Infrastructure in Antarctica' and the International Association of Geodesy Subcommission 1.3f 'Regional Reference Frame in Antarctica'. We would like to thank the editor, Adam Martin, as well as Matt King and an anonymous reviewer for their valuable comments which helped to improve the manuscript.

Author contributions **MS**: writing – original draft (lead), writing – review & editing (lead); **OE**: writing – original draft (equal), writing – review & editing (supporting); **EJOS**: writing – review & editing (supporting); **WVDW**: writing – review & editing (supporting); **MH**: writing – review & editing (supporting).

Funding We gratefully acknowledge the funding granted over many years by the different national funding agencies and national Antarctic programmes..

Data availability Data sharing is not applicable to this article as no datasets were generated or analysed during the current study.

References

Adie, R.J. 1962. The geology of Antarctica. *American Geophysical Union Geophysical Monograph Series*, **7**, 26–39, https://doi.org/10.1029/GM007p0026

Altamimi, Z., Rebischung, P., Métivier, L. and Collilieux, X. 2016. ITRF2014: a new release of the International Terrestrial Reference Frame modeling nonlinear station motions. *Journal of Geophysical Research: Solid Earth*, **121**, 6109–6131, https://doi.org/10.1002/2016JB013098

An, M., Wiens, D.A. *et al.* 2015*a*. S-velocity model and inferred Moho topography beneath the Antarctic plate from Rayleigh waves. *Journal of Geophysical Research: Solid Earth*, **120**, 359–383, https://doi.org/10.1002/2014JB011332

An, M., Wiens, D.A. *et al.* 2015*b*.Temperature, lithosphere–asthenosphere boundary, and heat flux beneath the Antarctic plate inferred from seismic velocities. *Journal of Geophysical Research: Solid Earth*, **120**, 8720–8742, https://doi.org/10.1002/2015JB011917

Aoyama, Y., Doi, K., Ikeda, H., Hayakawa, H. and Shibuya, K. 2016. Five years' gravity observation with the superconducting gravimeter OSG# 058 at Syowa Station, East Antarctica: gravitational effects of accumulated snow mass. *Geophysical Journal International*, **205**, 1290–1304, https://doi.org/10.1093/gji/ggw078

Argus, D.F. 2012. Uncertainty in the velocity between the mass center and surface of earth. *Journal of Geophysical Research: Solid Earth*, **117**, B10405, https://doi.org/10.1029/2012JB009196

Argus, D.F., Blewitt, G., Peltier, W.R. and Kreemer, C. 2011. Rise of the Ellsworth mountains and parts of the East Antarctic coast observed with GPS. *Geophysical Research Letters*, **38**, L16303, https://doi.org/10.1029/2011GL048025

Argus, D.F., Peltier, W.R., Drummond, R. and Moore, A.W. 2014. The Antarctica component of postglacial rebound model ICE-6G_C (VM5a) based on GPS positioning, exposure age dating of ice thicknesses, and relative sea level histories. *Geophysical Journal International*, **198**, 537–563, https://doi.org/10.1093/gji/ggu140

Barletta, V.R., Sabadini, R. and Bordoni, A. 2008. Isolating the PGR signal in the GRACE data: impact on mass balance estimates in Antarctica and Greenland. *Geophysical Journal International*, **172**, 18–30, https://doi.org/10.1111/j.1365-246X.2007.03630.x

Barletta, V.R., Bevis, M. *et al.* 2018. Observed rapid bedrock uplift in Amandsen Sea embayment promotes ice-sheet stability. *Science*, **360**, 1335–1339, https://doi.org/10.1126/science.aao1447

Barletta, V.R., Nield, G.A., van der Wal, W. and van Calcar, C.J. 2022. Glacial isostatic adjustment and postseismic deformation in Antarctica. *Geological Society, London, Memoirs*, **56**, in press.

Bevis, M., Kendrick, E. *et al*. 2009. Geodetic measurements of vertical crustal velocity in West Antarctica and the implications for ice mass balance. *Geochemistry, Geophysics, Geosystems*, **10**, Q10005, https://doi.org/10.1029/2009GC002642

Bevis, M., Wahr, J. *et al*. 2012. Bedrock displacements in Greenland manifest ice mass variations, climate cycles and climate change. *Proceedings of the National Academy of Sciences of the United States of America*, **109**, 11944–11948, https://doi.org/10.1073/pnas.1204664109

Bevis, M.C., Harig, S.A. *et al*. 2019. Accelerating changes in ice mass within Greenland, and the ice sheet's sensitivity to atmospheric forcing. *Proceedings of the National Academy of Sciences of the United States of America*, **116**, 1934–1939, https://doi.org/10.1073/pnas.1806562116

Blewitt, G. 2003. Self-consistency in reference frames, geocenter definition, and surface loading of the solid earth. *Journal of Geophysical Research: Solid Earth*, **108**, 2103, https://doi.org/10.1029/2002JB002082

Blewitt, G., Kreemer, C., Hammond, W.C. and Gazeaux, J. 2016. MIDAS robust trend estimator for accurate GPS station velocities without step detection. *Journal of Geophysical Research: Solid Earth*, **121**, 2054–2068, https://doi.org/10.1002/2015JB012552

Brenner, A.C., DiMarzio, J.P. and Zwally, H.J. 2007. Precision and accuracy of satellite radar and laser altimeter data over the continental ice sheets. *IEEE Transactions on Geoscience and Remote Sensing*, **45**, 321–331, https://doi.org/10.1109/TGRS.2006.887172

Bos, M.S., Fernandes, R.M.S., Williams, S.D.P. and Bastos, L. 2013. Fast error analysis of continuous GNSS observations with missing data. *Journal of Geodesy*, **87**, 351–360, https://doi.org/10.1007/s00190-012-0605-0

Bos, M.S., Penna, N.T., Baker, T.F. and Clarke, P.J. 2015. Ocean tide loading displacements in Western Europe: 2. GPS-observed anelastic dispersion in the asthenosphere. *Journal of Geophysical Research: Solid Earth*, **120**, 6540–6557, https://doi.org/10.1002/2015JB011884

Bouman, J., Fuchs, M., Ivins, E.V., Van Der Wal, W., Schrama, E., Visser, P.N.A.M. and Horwath, M. 2014. Antarctic outlet glacier mass change resolved at basin scale from satellite gravity gradiometry. *Geophysical Research Letters*, **41**, 5919–5926, https://doi.org/10.1002/2014GL060637

Burov, E.B. 2011. Rheology and strength of the lithosphere. *Marine and Petroleum Geology*, **28**, 1402–1443, https://doi.org/10.1016/j.marpetgeo.2011.05.008

Busch, P., Scheinert, M. *et al*. 2017. GNSS measurements in West Antarctica to reconcile glacial-isostatic adjustment. Presented at the IAG/SCAR-SERCE Workshop on Glacial Isostatic Adjustment and Elastic Deformation, 5–7 September 2017, Reykjavik, Iceland.

Caron, L. and Ivins, E.R. 2020. A baseline Antarctic GIA correction for space gravimetry. *Earth and Planetary Science Letters*, **531**, 115957, https://doi.org/10.1016/j.epsl.2019.115957

Caron, L., Ivins, E.R., Larour, E., Adhikari, S., Nilsson, J. and Blewitt, G. 2018. GIA model statistics for GRACE hydrology, cryosphere, and ocean science. *Geophysical Research Letters*, **45**, 2203–2212, https://doi.org/10.1002/2017GL076644

Chen, J.L., Wilson, C.R., Blankenship, D.D. and Tapley, B.D. 2006. Antarctic mass rates from GRACE. *Geophysical Research Letters*, **33**, L11502, https://doi.org/10.1029/2006GL026369

Chen, J.L., Wilson, C.R., Tapley, B.D. and Grand, S. 2007. GRACE detects coseismic and postseismic deformation from the Sumatra-Andaman earthquake. *Geophysical Research Letters*, **34**, L13302, https://doi.org/10.1029/2007GL030356

Cheng, M.K., Eanes, R.J., Shum, C.K., Schutz, B.E. and Tapley, B.D. 1989. Temporal variations in low degree zonal harmonics from Starlette orbit analysis. *Geophysical Research Letters*, **16**, 393–396, https://doi.org/10.1029/GL016i005p00393

Dahle, C. 2020. *Release Notes for GFZ GRACE-FO Level-2 Products – version RL06*. GFZ German Research Centre for Geosciences, Potsdam Germany.

Dietrich, R. (ed.) 1996. *The Geodetic Antarctic Project GAP95. German Contributions to the SCAR 95 Epoch Campaign. Deutsche Geodätische Kommission, B 304*. Bayerischen Akademie der Wissenschaften, München, Germany.

Dietrich, R. (ed.) 2000. *Deutsche Beiträge zu GPS-Kampagnen des Scientific Committee on Antarctic Research (SCAR) 1995–1998, Deutsche Geodätische Kommission, B310*. Bayerischen Akademie der Wissenschaften, München, Germany.

Dietrich, R. and Rülke, A. 2008. A precise reference frame for Antarctica from SCAR GPS campaign data and some geophysical implications. *In*: Capra, A. and Dietrich, R. (eds) *Geodetic and Geophysical Observations in Antarctica*. Springer, Berlin, 1–10.

Dietrich, R., Dach, R. *et al*. 2001. ITRF coordinates and plate velocities from repeated GPS campaigns in Antarctica – an analysis based on different individual solutions. *Journal of Geodesy*, **74**, 756–766, https://doi.org/10.1007/s001900000147

Dietrich, R., Rülke, A. *et al*. 2004. Plate kinematics and deformation status of the Antarctic Peninsula based on GPS. *Global and Planetary Change*, **42**, 313–321, https://doi.org/10.1016/j.gloplacha.2003.12.003

Dill, R., Klemann, V., Martinec, Z. and Tesauro, M. 2015. Applying local Green's functions to study the influence of the crustal structure on hydrological loading displacements. *Journal of Geodynamics*, **88**, 14–22, https://doi.org/10.1016/j.jog.2015.04.005

Dobslaw, H., Bergmann-Wolf, I. *et al*. 2017. A new high-resolution model of non-tidal atmosphere and ocean mass variability for de-aliasing of satellite gravity observations: AOD1B RL06. *Geophysical Journal International*, **211**, 263–269, https://doi.org/10.1093/gji/ggx302

Donnellan, A. and Luyendyk, B.P. 2004. GPS evidence for a coherent Antarctic plate and for postglacial rebound in Marie Byrd Land. *Global and Planetary Change*, **42**, 305–311, https://doi.org/10.1016/j.gloplacha.2004.02.006

Dziewonski, A.M. and Anderson, D.L. 1981. Preliminary reference earth model. *Physics of the Earth and Planetary Interiors*, **25**, 297–356, https://doi.org/10.1016/0031-9201(81)90046-7

Engels, O. 2020. Stochastic modelling of geophysical signal constituents within a kalman filter framework. *In*: Montillet, J.P. and Bos, M. (eds) *Geodetic Time Series Analysis in Earth Sciences*. Springer Geophysics. Springer, Cham, Switzerland, 239–260, https://doi.org/10.1007/978-3-030-21718-1_8

Engels, O., Gunter, B.C., Riva, R.E.M. and Klees, R. 2018. Separating geophysical signals using GRACE and high-resolution data: A case study in Antarctica. *Geophysical Research Letters*, **45**, 12 340–12 349, https://doi.org/10.1029/2018GL079670

Farrell, W.E. 1972. Deformation of the earth by surface loads. *Review of Geophysics*, **10**, 761–797, https://doi.org/10.1029/RG010i003p00761

Foley, S.F., Andronikov, A.V., Halpin, J.A., Daczko, N.R. and Jacob, D.E. 2021. Mantle rocks in East Antarctica. *Geological Society, London, Memoirs*, **56**, https://doi.org/10.1144/M56-2020-8

Geruo, A., Wahr, J. and Zhong, S. 2013. Computations of the viscoelastic response of a 3-D compressible Earth to surface loading: an application to Glacial Isostatic Adjustment in Antarctica and Canada. *Geophysical Journal International*, **192**, 557–572, https://doi.org/10.1093/gji/ggs030

Ghelichkhan, S., Murböck, M., Colli, L., Pail, R. and Bunge, H.P. 2018. On the observability of epeirogenic movement in current and future gravity missions. *Gondwana Research*, **53**, 273–284, https://doi.org/10.1016/j.gr.2017.04.016

Gomez, N., Latychev, K. and Pollard, D. 2018. A coupled ice sheet–sea level model incorporating 3D Earth structure: Variations in Antarctica during the last deglacial retreat. *Journal of Climate*, **31**, 4041–4054, https://doi.org/10.1175/JCLI-D-17-0352.1

Groh, A., Ewert, H. *et al*. 2012. An investigation of glacial isostatic adjustment over the Amundsen Sea sector, West Antarctica. *Global and Planetary Change*, **98–99**, 45–53, https://doi.org/10.1016/j.gloplacha.2012.08.001

Groh, A., Ewert, H. *et al*. 2014. Mass, volume and velocity of the Antarctic ice sheet: present-day changes and error effects. *Surveys in Geophysics*, **35**, 1481–1505, https://doi.org/10.1007/s10712-014-9286-y

Gunter, B., Didova, O. *et al*. 2014. Empirical estimation of present-day antarctic glacial isostatic adjustment and ice mass change. *The Cryosphere*, **8**, 743–760, https://doi.org/10.5194/tc-8-743-2014

Han, S.C., Sauber, J. and Pollitz, F. 2016. Postseismic gravity change after the 2006–2007 great earthquake doublet and constraints on the asthenosphere structure in the central Kuril Islands. *Geophysical Research Letters*, **43**, 3169–3177, https://doi.org/10.1002/2016GL068167

Handler, M.R., Wysoczanski, R.J. and Gamble, J.A. 2021. Marie Byrd Land lithospheric mantle: a review of the xenolith record. *Geological Society, London, Memoirs*, **56**, https://doi.org/10.1144/M56-2020-17

Harig, C. and Simons, F.J. 2015. Accelerated West Antarctic ice mass loss continues to outpace East Antarctic gains. *Earth and Planetary Science Letters*, **415**, 134–141, https://doi.org/10.1016/j.epsl.2015.01.029

Hermans, T.H.J., van der Wal, W. and Broerse, T. 2018. Reversal of the direction of horizontal velocities induced by GIA as a function of mantle viscosity. *Geophysical Research Letters*, **45**, 9597–9604, https://doi.org/10.1029/2018GL078533

Horwath, M. and Dietrich, R. 2009. Signal and error in mass change inferences from GRACE: the case of Antarctica. *Geophysical Journal International*, **177**, 849–864, https://doi.org/10.1111/j.1365-246X.2009.04139.x

Hu, Y. and Freymueller, J.T. 2019. Geodetic observations of time variable glacial isostatic adjustment in Southeast Alaska and its implications for Earth rheology. *Journal of Geophysical Research: Solid Earth*, **124**, 9870–9889, https://doi.org/10.1029/2018JB017028

Ivins, E.R. and James, T.S. 2005. Antarctic glacial isostatic adjustment: a new assessment. *Antarctic Science*, **17**, 541–553, https://doi.org/10.1017/S0954102005002968

Ivins, E.R., James, T.S., Wahr, J., Schrama, E.J.O., Landerer, F.W. and Simon, K.M. 2013. Antarctic contribution to sea level rise observed by GRACE with improved GIA correction. *Journal of Geophysical Research: Solid Earth*, **118**, 3126–3141, https://doi.org/10.1002/jgrb.50208

Ivins, E.R., Caron, L., Adhikari, S., Larour, E. and Scheinert, M. 2020. A linear viscoelasticity for decadal to centennial time scale mantle deformation. *Reports on Progress in Physics*, **83**, 106801, https://doi.org/10.1088/1361-6633/aba346

Ivins, E.R., van der Wal, W., Wiens, D.A., Lloyd, A.J. and Caron, L. 2021. Antarctic upper-mantle rheology. *Geological Society, London, Memoirs*, **56**, https://doi.org/10.1144/M56-2020-19

Jacobs, J., Elburg, M. *et al*. 2015. Two distinct Late Mesoproterozoic/Early Neoproterozoic basement provinces in central/eastern Dronning Maud Land, East Antarctica: The missing link, 15–21° E. *Precambrian Research*, **265**, 249–272, https://doi.org/10.1016/j.precamres.2015.05.003

Jiang, Y., Wu, X., van den Broeke, M.R., Munneke, P.K., Simonsen, S.B., van der Wal, W. and Vermeersen, B.L. 2021. Assessing global present-day surface mass transport and glacial isostatic adjustment from inversion of geodetic observations. *Journal of Geophysical Research: Solid Earth*, **126**, e2020JB020713, https://doi.org/10.1029/2020JB020713

Kang, K., Wahr, J., Heflin, M. and Desai, S. 2015. Stacking global GPS verticals and horizontals to solve for the fortnightly and monthly body tides: implications for mantle anelasticity. *Journal of Geophysical Research: Solid Earth*, **120**, 1787–1803, https://doi.org/10.1002/2014JB011572

King, M.A. and Santamaría-Gómez, A. 2016. Ongoing deformation of Antarctica following recent Great Earthquakes. *Geophysical Research Letters*, **43**, 1918–1927, https://doi.org/10.1002/2016GL067773

King, M.A., Altamimi, Z. *et al*. 2010. Improved constraints on models of glacial isostatic adjustment: a review of the contribution of ground-based geodetic observations. *Surveys in Geophysics*, **31**, 465–507, https://doi.org/10.1007/s10712-010-9100-4

King, M.A., Bingham, R.J., Moore, P., Whitehouse, P.L., Bentley, M.J. and Milne, G.A. 2012. Lower satellite-gravimetry estimates of Antarctic sea-level contribution. *Nature*, **491**, 586–589, https://doi.org/10.1038/nature11621

Koch, A., Sanjuan, J., Gohlke, M., Mahrdt, C., Brause, N., Braxmaier, C. and Heinzel, G. 2018. Line of sight calibration for the laser ranging interferometer on-board the GRACE follow-on mission: on-ground experimental validation. *Optics Express*, **26**, 25892–25908, https://doi.org/10.1364/OE.26.025892

Konfal, S., Kendrick, E., Saddler, D., Wilson, T. and Bevis, M. 2016. Crustal velocity solutions in polar environments: GPS position errors caused by ice in antennas. Presented at the XXXIV SCAR Meeting and Open Science Conference, 19–31 August 2016, Kuala Lumpur, Malaysia.

Konfal, S.A., Wilson, T.J.W. *et al*. 2018. Utilizing GPS to investigate past ice mass change in the Ross Sea region, Antarctica. *AGU Fall Meeting Abstracts*, **2018**, G43B-0716, https://ui.adsabs.harvard.edu/abs/2018AGUFM.G43B0716K

Koulali, A. and Clarke, P.J. 2020. Effect of antenna snow intrusion on vertical GPS position time series in Antarctica. *Journal of Geodesy*, **94**, 101, https://doi.org/10.1007/s00190-020-01403-6

Kusche, J., Schmidt, R., Petrovic, S. and Rietbroek, R. 2009. Decorrelated GRACE time-variable gravity solutions by GFZ, and their validation using a hydrological model. *Journal of Geodesy*, **83**, 903–913, https://doi.org/10.1007/s00190-009-0308-3

Kvas, A. and Mayer-Gürr, T. 2019. GRACE gravity field recovery with background model uncertainties. *Journal of Geodesy*, **93**, 2543–2552, https://doi.org/10.1007/s00190-019-01314-1

Landerer, F.W. and Swenson, S.C. 2012. Accuracy of scaled GRACE terrestrial water storage estimates. *Water Resources Research*, **48**, W04531, https://doi.org/10.1029/2011WR011453, w04531

Landerer, F.W., Flechtner, F.M. *et al*. 2020. Extending the global mass change data record: GRACE follow-on instrument and science data performance. *Geophysical Research Letters*, **47**, e2020GL088306, https://doi.org/10.1029/2020GL088306

Lange, H., Casassa, G. *et al*. 2014. Observed crustal uplift near the Southern Patagonian Icefield constrains improved viscoelastic Earth models. *Geophysical Research Letters*, **41**, 805–812, https://doi.org/10.1002/2013GL058419

Larour, E., Seroussi, H., Adhikari, S., Ivins, E., Caron, L., Morlighem, M. and Schlegel, N. 2019. Slowdown in Antarctic mass loss from solid Earth and sea-level feedbacks. *Science*, **364**, 6444, https://doi.org/10.1126/science.aav7908

Lenaerts, J.T.M., van den Broeke, M.R., van de Berg, W.J., van Meijgaard, E. and Kuipers Munneke, P. 2012. A new, high-resolution surface mass balance map of Antarctica 1979–2010) based on regional atmospheric climate modeling. *Geophysical Research Letters*, **39**, L04501, https://doi.org/10.1029/2011GL050713

Ligtenberg, S.R.M., Helsen, M.M. and van den Broeke, M.R. 2011. An improved semi-empirical model for the densification of Antarctic firn. *The Cryosphere*, **5**, 809–819, https://doi.org/10.5194/tc-5-809-2011

Ligtenberg, S.R.M., Horwath, M., van den Broeke, M.R. and Legrésy, B. 2012. Quantifying the seasonal 'breathing' of the Antarctic ice sheet. *Geophysica. Research Letters*, **39**, L23501, https://doi.org/10.1029/2012GL053628

Liu, B., King, M. and Dai, W. 2018. Common mode error in Antarctic GPS coordinate time-series on its effect on bedrock-uplift estimates. *Geophysical Journal International*, **214**, 1652–1664, https://doi.org/10.1093/gji/ggy217

Lloyd, A.J., Wiens, D.A. *et al*. 2020. Seismic structure of the Antarctic upper mantle imaged with adjoint tomography. *Journal of Geophysical Research: Solid Earth*, **125**, https://doi.org/10.1029/2019JB017823

Loomis, B.D., Luthcke, S.B. and Sabaka, T.J. 2019. Regularization and error characterization of GRACE mascons. *Journal of Geodesy*, **93**, 1381–1398, https://doi.org/10.1007/s00190-019-01252-y

Mäkinen, J., Amalvict, M., Shibuya, K. and Fukuda, Y. 2007. Absolute gravimetry in Antarctica: status and prospects. *Journal of Geodynamics*, **43**, 339–357, https://doi.org/10.1016/j.jog.2006.08.002

Marderwald, E.R., Aragon Paz, J.M.A. *et al*. 2020. Perito Moreno Glacier dam rupture – a recurrent natural experiment to probe solid-earth elasticity. *Journal of South American Earth Sciences*, **104**, 102904, https://doi.org/10.1016/j.jsames.2020.102904

Martin, A.P., Cooper, A.F., Price, R.C., Doherty, C.L. and Gamble, J.A. 2021. A review of mantle xenoliths in volcanic rocks from southern Victoria Land, Antarctica. *Geological Society, London, Memoirs*, **56**, https://doi.org/10.1144/M56-2019-42

Martín-Español, A., King, M.A., Zammit-Mangion, A., Andrews, B., Moore, P. and Bamber, J.L. 2016*a*. An assessment of forward and inverse GIA solutions for Antarctica. *Journal of Geophysical Research: Solid Earth*, **121**, 6947–6965, https://doi.org/10.1002/2016JB013154

Martín-Español, A., Zammit-Mangion, A. *et al*. 2016*b*. Spatial and temporal Antarctic Ice Sheet mass trends, glacio-isostatic adjustment, and surface processes from a joint inversion of satellite altimeter, gravity, and GPS data. *Journal of Geophysical Research: Earth Surface*, **121**, 182–200, https://doi.org/10.1002/2015JF003550

Mayer-Gürr, T., Behzadpur, S., Ellmer, M., Kvas, A., Klinger, B., Strasser, S. and Zehentner, N. 2018. *ITSG-Grace2018 – Monthly, Daily and Static Gravity Field Solutions from GRACE*. GFZ Data Services, https://doi.org/10.5880/ICGEM.2018.003; model data also available at https://www.tugraz.at/institute/ifg/downloads/gravity-field-models/

Mieth, M. and Jokat, W. 2014. New aeromagnetic view of the geological fabric of southern Dronning Maud Land and Coats Land, East Antarctica. *Gondwana Research*, **25**, 358–367, https://doi.org/10.1016/j.gr.2013.04.003

Mitrovica, J.X., Milne, G.A. and Davis, J.L. 2001. Glacial isostatic adjustment on a rotating earth. *Geophysical Journal International*, **147**, 562–578, https://doi.org/10.1046/j.1365-246x.2001.01550.x

Nield, G.A., Whitehouse, P.L., King, M.A., Clarke, P.J. and Bentley, M.J. 2012. Increased ice loading in the Antarctic Peninsula since the 1850s and its effect on glacial isostatic adjustment. *Geophysical Research Letters*, **39**, L17504, https://doi.org/10.1029/2012gl052559

Nield, G.A., Barletta, V.R. *et al*. 2014. Rapid bedrock uplift in the Antarctic Peninsula explained by viscoelastic response to recent ice unloading. *Earth and Planetary Science Letters*, **397**, 32–41, https://doi.org/10.1016/j.epsl.2014.04.019

Nield, G.A., Whitehouse, P.L., King, M.A. and Clarke, P.J. 2016. Glacial isostatic adjustment in response to changing Late Holocene behaviour of ice streams on the Siple Coast, West Antarctica. *Geophysical Journal International*, **205**, 1–21, https://doi.org/10.1093/gji/ggv532

Nield, G.A., Whitehouse, P.L., van der Wal, W., Blank, B., O'Donnell, J.P. and Stuart, G.W. 2018. The impact of lateral variations in lithospheric thickness on glacial isostatic adjustment in West Antarctica. *Geophysical Journal International*, **214**, 811–824, https://doi.org/10.1093/gji/ggy158

Nielsen, K., Khan, S.A., Spada, G., Wahr, J., Bevis, M., Liu, L. and van Dam, T. 2013. Vertical and horizontal surface displacements near Jakobshavn Isbræ driven by melt-induced and dynamic ice loss. *Journal of Geophysical Research: Solid Earth*, **118**, 1837–1844, https://doi.org/10.1002/jgrb.50145

Pappa, F. and Ebbing, J. 2021. Gravity, magnetics and geothermal heat flow of the Antarctic lithospheric crust and mantle. *Geological Society, London, Memoirs*, **56**, https://doi.org/10.1144/M56-2020-5

Peidou, A. and Pagiatakis, S. 2020. Stripe mystery in GRACE geopotential models revealed. *Geophysical Research Letters*, **47**, e2019GL085497, https://doi.org/10.1029/2019GL085497

Peltier, W.R. 1998. Postglacial variations in the level of the sea: Implications for climate dynamics and solid-Earth geophysics. *Reviews of Geophysics*, **36**, 603–689, https://doi.org/10.1029/98RG02638

Peltier, W.R. 2004. Global glacial isostasy and the surface of the ice-age earth: the ICE-5G (VM2) model and GRACE. *Annual Review of Earth and Planetary Science*, **32**, 111–149, https://doi.org/10.1146/annurev.earth.32.082503.144359

Ranalli, G. 1995. *Rheology of the Earth*. 2nd edn. Chapman & Hall, London.

Raymond, C.A., Ivins, E.R., Heflin, M.B. and James, T.S. 2004. Quasi-continuous global positioning system measurements of glacial isostatic deformation in the Northern Transantarctic Mountains. *Global and Planetary Change*, **42**, 295–303, https://doi.org/10.1016/j.gloplacha.2003.11.013

Rebischung, P., Altamimi, Z., Ray, J. and Garayt, B. 2016. The IGS contribution to ITRF2014. *Journal of Geodesy*, **90**, 611–630, https://doi.org/10.1007/s00190-016-0897-6

Riddell, A.R., King, M.A., Watson, C.S., Sun, Y., Riva, R.E.M. and Rietbroek, R. 2017. Uncertainty in geocenter estimates in the context of ITRF2014. *Journal of Geophysical Research: Solid Earth*, **122**, 4020–4032, https://doi.org/10.1002/2016JB013698

Rietbroek, R., Brunnabend, S.E., Kusche, J., Schröter, J. and Dahle, C. 2016. Revisiting the contemporary sea-level budget on global and regional scales. *Proceedings of the National Academy of Sciences of the United States of America*, **113**, 1504–1509, https://doi.org/10.1073/pnas.1519132113

Riva, R.E.M., Gunter, B.C. *et al*. 2009. Glacial isostatic adjustment over Antarctica from combined ICESat and GRACE satellite data. *Earth and Planetary Science Letters*, **288**, 516–523, https://doi.org/10.1016/j.epsl.2009.10.013

Rülke, A. 2009. *Zur Realisierung eines terrestrischen Referenzsystems in globalen und regionalen GPS-Netzen*. PhD thesis, TU Dresden, http://nbn-resolving.de/urn:nbn:de:bsz:14-qucosa-24543

Rülke, A., Dietrich, R., Fritsche, M., Rothacher, M. and Steigenberger, P. 2008. Realization of the Terrestrial Reference System by a reprocessed global GPS network. *Journal of Geophysical Research: Solid Earth*, **113**, B08403, https://doi.org/10.1029/2007JB005231

Rülke, A., Dietrich, R. *et al*. 2015. The Antarctic regional GPS network densification: status and results. *In*: Rizos, C. and Willis, P. (eds) *IAG 150 Years*. International Association of Geodesy Symposia, **143**. Springer, Cham, Switzerland, 133–139, https://doi.org/10.1007/1345_2015_79

Sasgen, I., Martinec, Z. and Fleming, K. 2007. Regional ice-mass changes and glacial-isostatic adjustment in Antarctica from GRACE. *Earth and Planetary Science Letters*, **264**, 391–401, https://doi.org/10.1016/j.epsl.2007.09.029

Sasgen, I., Konrad, H., Ivins, E.R., van den Broeke, M.R., Bamber, J.L., Martinec, Z. and Klemann, V. 2013. Antarctic ice-mass balance 2003 to 2012: regional reanalysis of GRACE satellite gravimetry measurements with improved estimate of glacial-isostatic adjustment based on GPS uplift rates. *The Cryosphere*, **7**, 1499–1512, https://doi.org/10.5194/tc-7-1499-2013

Sasgen, I., Martín-Español, A. *et al*. 2017. Joint inversion estimate of regional glacial isostatic adjustment in Antarctica considering a lateral varying earth structure (ESA STSE project REGINA). *Geophysical Journal International*, **211**, 1534–1553, https://doi.org/10.1093/gji/ggx368

Sasgen, I., Martín-Español, A. *et al*. 2018. Altimetry, gravimetry, GPS and viscoelastic modeling data for the joint inversion for glacial isostatic adjustment in Antarctica (ESA STSE project REGINA). *Earth System Science Data*, **10**, 493–523, https://doi.org/10.5194/essd-10-493-2018

Schoen, N., Zammit-Mangion, A., Rougier, J., Flament, T., Rémy, F., Luthcke, S. and Bamber, J. 2015. Simultaneous solution for mass trends on the West Antarctic Ice Sheet. *The Cryosphere*, **9**, 805–819, https://doi.org/10.5194/tc-9-805-2015

Schrama, E.J.O., Wouters, B. and Rietbroek, R. 2014. A mascon approach to assess ice sheet and glacier mass balances and their uncertainties from GRACE data. *Journal of Geophysical Research: Solid Earth*, **119**, 6048–6066, https://doi.org/10.1002/2013JB010923

Schröder, L., Horwath, M., Dietrich, R., Helm, V., van den Broeke, M.R. and Ligtenberg, S.R.M. 2019*a*. Four decades of Antarctic surface elevation changes from multi-mission satellite altimetry. *The Cryosphere*, **13**, 427–449, https://doi.org/10.5194/tc-13-427-2019

Schröder, L., Horwath, M., Dietrich, R., Helm, V., van den Broeke, M.R., and Ligtenberg, S.R.M. 2019*b*. Gridded surface elevation changes from multi-mission satellite altimetry 1978–2017. *PANGAEA*, https://doi.org/10.1594/PANGAEA.897390

Seo, K.W., Wilson, C.R., Chen, J. and Waliser, D.E. 2008. GRACE's spatial aliasing error. *Geophysical Journal International*, **172**, 41–48, https://doi.org/10.1111/j.1365-246X.2007.03611.x

Shepherd, A., Ivins, E. *et al*. 2018. Mass balance of the Antarctic Ice Sheet from 1992 to 2017. *Nature*, **558**, 219–222, https://doi.org/10.1038/s41586-018-0179-y

Shepherd, A., Ivins, E. *et al*. 2020. Mass balance of the Greenland Ice Sheet from 1992 to 2018. *Nature*, **579**, 233–239, https://doi.org/10.1038/s41586-019-1855-2

Spada, G. 2017. Glacial isostatic adjustment and contemporary sea level rise: an overview. *Surveys in Geophysics*, **38**, 153–185, https://doi.org/10.1007/s10712-016-9379-x

Steinberger, B. and Becker, T.W. 2018. A comparison of lithospheric thickness models. *Tectonophysics*, **746**, 325–338, https://doi.org/10.1016/j.tecto.2016.08.001

Swenson, S. and Wahr, J. 2002. Methods for inferring regional surface-mass anomalies from Gravity Recovery and Climate Experiment (GRACE) measurements of time-variable gravity. *Journal of Geophysical Research: Solid Earth*, **107**, 2193, https://doi.org/10.1029/2001JB000576

Swenson, S. and Wahr, J. 2006. Post-processing removal of correlated errors in GRACE data. *Geophysical Research Letters*, **33**, L08402, https://doi.org/10.1029/2005GL025285

Tamisiea, M.E., Mitrovica, J.X. and Davis, J.L. 2007. GRACE gravity data constrain ancient ice geometries and continental dynamics over Laurentia. *Science*, **316**, 881–883, https://doi.org/10.1126/science.1137157

Tapley, B.D., Bettadpur, S., Ries, J.C., Thompson, P.F. and Watkins, M.M. 2004. GRACE measurements of mass variability in the Earth system. *Science*, **305**, 503–505, https://doi.org/10.1126/science.1099192

Thomas, I.D., King, M.A. *et al*. 2011. Widespread low rates of Antarctic glacial isostatic adjustment revealed by GPS observations. *Geophysical Research Letters*, **38**, L22302, https://doi.org/10.1029/2011GL049277

Tregoning, P., Twilley, B., Hendy, M. and Zwartz, D. 1999. Monitoring isostatic rebound in Antarctica using continuous remote GPS observations. *GPS Solutions*, **2**, 70–75, https://doi.org/10.1007/PL00012759

Tregoning, P., Welsh, A., McQueen, H. and Lambeck, K. 2000. The search for postglacial rebound near the Lambert Glacier, Antarctica. *Earth, Planets and Space*, **52**, 1037–1041, https://doi.org/10.1186/BF03352327

Turner, R.J., Reading, A.M. and King, M.A. 2020. Separation of tectonic and local components of horizontal GPS station velocities: a case study for glacial isostatic adjustment in East Antarctica. *Geophysical Journal International*, **222**, 1555–1569, https://doi.org/10.1093/gji/ggaa265

Van Camp, M., de Viron, O., Watlet, A., Meurers, B., Francis, O. and Caudron, C. 2017. Geophysics from terrestrial time-variable gravity measurements. *Reviews of Geophysics*, **55**, 938–992. https://doi.org/10.1002/2017RG000566

van der Wal, W., Barnhoorn, A., Stocchi, P., Gradmann, S., Wu, P., Drury, M. and Vermeersen, B. 2013. Glacial isostatic adjustment model with composite 3-D Earth rheology for Fennoscandia. *Geophysical Journal International*, **194**, 61–77, https://doi.org/10.1093/gji/ggt099

van der Wal, W., Whitehouse, P.L. and Schrama, E.J.O. 2015. Effect of GIA models with 3D composite mantle viscosity on GRACE mass balance estimates for Antarctica. *Earth and Planetary Science Letters*, **414**, 134–143, https://doi.org/10.1016/j.epsl.2015.01.001

Vazquez Becerra, G.E. 2009. *Geodesy in Antarctica: A Pilot Study Based on the TAMDEF GPS Network, Victoria Land, Antarctica*. Ohio State University, Geodetic Science and Surveying Report 492, https://kb.osu.edu/handle/1811/78631

Velicogna, I. 2009. Increasing rates of ice mass loss from the Greenland and Antarctic ice sheets revealed by GRACE. *Geophysical Research Letters*, **36**, L19503, https://doi.org/10.1029/2009GL040222

Velicogna, I. and Wahr, J. 2002. A method for separating Antarctic postglacial rebound and ice mass balance using future ICESat geoscience laser altimeter system, Gravity Recovery and Climate Experiment, and GPS satellite data. *Journal of Geophysical Research: Solid Earth*, **107**, 2263, https://doi.org/10.1029/2001JB000708

Velicogna, I. and Wahr, J. 2006. Measurements of time-variable gravity show mass loss in Antarctica. *Science*, **311**, 1754–1756, https://doi.org/10.1126/science.1123785

Velicogna, I., Mohajerani, Y.E. *et al*. 2020. Continuity of ice sheet mass loss in Greenland and Antarctica from the GRACE and GRACE follow-on missions. *Geophysical Research Letters*, **47**, e2020GL087291, https://doi.org/10.1029/2020GL087291

Villiger, A. and Dach, R. (eds) 2020. *International GNSS Service: Technical Report 2019*. IGS Central Bureau and University of Bern Open Publishing, https://doi.org/10.7892/boris.144003

Wahr, J., Wingham, D. and Bentley, C. 2000. A method of combining ICESat and GRACE satellite data to constrain Antarctic mass balance. *Journal of Geophysical Research: Solid Earth*, **105**, 16 279–16 294, https://doi.org/10.1029/2000JB900113

Wahr, J., Swenson, S. and Velicogna, I. 2006. Accuracy of GRACE mass estimates. *Geophysical Research Letters*, **33**, L06401, https://doi.org/10.1029/2005GL025305

Whitehouse, P.L., Bentley, M.J., Milne, G.A., King, M.A. and Thomas, I.D. 2012. A new glacial isostatic adjustment model for Antarctica: calibrated and tested using observations of relative sea-level change and present-day uplift rates. *Geophysical Journal International*, **190**, 1464–1482, https://doi.org/10.1111/j.1365-246X.2012.05557.x

Whitehouse, P.L. 2018. Glacial isostatic adjustment modelling: historical perspectives, recent advances, and future directions. *Earth Surface Dynamics*, **6**, 401–429, https://doi.org/10.5194/esurf-6-401-2018

Wiens, D.A., Shen, W. and Lloyd, A.J. 2021. The seismic structure of the Antarctic upper mantle. *Geological Society, London, Memoirs*, **56**, https://doi.org/10.1144/M56-2020-18

Wiese, D.N., Landerer, F.W. and Watkins, M.M. 2016. Quantifying and reducing leakage errors in the JPL RL05M GRACE mascon solution. *Water Resources Research*, **52**, 7490–7502, https://doi.org/10.1002/2016WR019344

Willen, M.O., Horwath, M., Schröder, L., Groh, A., Ligtenberg, S.R.M., Kuipers Munneke, P. and van den Broeke, M.R. 2020. Sensitivity of inverse glacial isostatic adjustment estimates over Antarctica. *The Cryosphere*, **14**, 349–366, https://doi.org/10.5194/tc-14-349-2020, https://tc.copernicus.org/articles/14/349/2020/

Williams, D.P. 2003. The effect of coloured noise on the uncertainties of rates estimated from geodetic time series. *Journal of Geodesy*, **76**, 483–494, https://doi.org/10.1007/s00190-002-0283-4

Williams, D.P. 2008. CATS: GPS coordinate time series analysis software. *GPS Solutions*, **12**, 147–153, https://doi.org/10.1007/s10291-007-0086-4

Williams, S.D.P., Moore, P., King, M.A. and Whitehouse, P.L. 2014. Revisiting GRACE Antarctic ice mass trends and accelerations considering autocorrelation. *Earth and Planetary Science Letters*, **385**, 12–21, https://doi.org/10.1016/j.epsl.2013.10.016

Wilson, T., Bevis, M. *et al*. 2019. Understanding themismatch between measured and model-predicted crustal motions across West Antarctica: Insights from POLENET-ANET GPS results. Presented at the Workshop on Glacial Isostatic Adjustment, Ice Sheets, and Sea-level Change – Observations, Analysis, and Modelling, 24–26 September 2019, Ottawa, Canada.

Wolstencroft, M., King, M.A. *et al*. 2015. Uplift rates from a new high-density GPS network in Palmer Land indicate significant late Holocene ice loss in the southwestern Weddell Sea. *Geophysical Journal International*, **203**, 737–754, https://doi.org/10.1093/gji/ggv327

Wouters, B., Bonin, J.A., Chambers, D.P., Riva, R.E., Sasgen, I. and Wahr, J. 2014. GRACE, time-varying gravity, Earth system dynamics and climate change. *Reports on Progress in Physics*, **77**, 116801, https://doi.org/10.1088/0034-4885/77/11/116801

Wu, X., Heflin, M.B. *et al*. 2010. Simultaneous estimation of global present-day water transport and glacial isostatic adjustment. *Nature Geoscience*, **3**, 642–646, https://doi.org/10.1038/ngeo938

Zammit-Mangion, A., Bamber, J.L., Schoen, N.W. and Rougier, J.C. 2015. A data-driven approach for assessing ice-sheet mass balance in space and time. *Annals of Glaciology*, **56**, 175–183, https://doi.org/10.3189/2015AoG70A021

Zanutta, A., Negusini, M. *et al*. 2017. Monitoring geodynamic activity in the Victoria Land, East Antarctica: evidence from GNSS measurements. *Journal of Geodynamics*, **110**, 31–42, https://doi.org/10.1016/j.jog.2017.07.008

Zanutta, A., Negusini, M. *et al*. 2018. New geodetic and gravimetric maps to infer geodynamics of Antarctica with insights on Victoria Land. *Remote Sensing*, **10**, 1608, https://doi.org/10.3390/rs10101608